

**A peer-reviewed version of this preprint was published in PeerJ on 15 August 2017.**

[View the peer-reviewed version](https://peerj.com/articles/3650) (peerj.com/articles/3650), which is the preferred citable publication unless you specifically need to cite this preprint.

Hautier L, Billet G, de Thoisy B, Delsuc F. 2017. Beyond the carapace: skull shape variation and morphological systematics of long-nosed armadillos (genus *Dasypus*) PeerJ 5:e3650  
<https://doi.org/10.7717/peerj.3650>

# Beyond the carapace: skull shape variation and morphological systematics of long-nosed armadillos (genus *Dasypus*)

Lionel Hautier <sup>Corresp., 1,2</sup>, Guillaume Billet <sup>3</sup>, Benoit De Thoisy <sup>4</sup>, Frédéric Delsuc <sup>1</sup>

<sup>1</sup> Institut des Sciences de l'Evolution de Montpellier, Université de Montpellier, Montpellier, France

<sup>2</sup> Mammal Section, Life Sciences, Vertebrate Division, The Natural History Museum, London, United Kingdom

<sup>3</sup> Muséum national d'Histoire naturelle, Paris, France

<sup>4</sup> Institut Pasteur de la Guyane, Cayenne, France

Corresponding Author: Lionel Hautier

Email address: lionel.hautier@umontpellier.fr

**Background.** The systematics of long-nosed armadillos (genus *Dasypus*) has been mainly based on a handful of external morphological characters and classical measurements. Here, we studied the pattern of morphological variation in the skull of long-nosed armadillos species, with a focus on the systematics of the widely distributed nine-banded armadillo (*D. novemcinctus*). **Methods.** We present the first exhaustive 3D comparison of the skull morphology within the genus *Dasypus*, based on  $\mu$ CT-scans. We used geometric morphometric approaches to explore the patterns of the intra- and interspecific morphological variation of the skull with regard to several factors such as taxonomy, geography, allometry, and sexual dimorphism. **Results.** We show that the shape and size of the skull vary greatly between *Dasypus* species, with *D. pilosus* representing a clear outlier compared to other long-nosed armadillos. The study of the cranial intraspecific variation in *D. novemcinctus* evidences clear links to the geographic distribution and argue in favour of a revision of past taxonomic delimitations. Our detailed morphometric comparisons detected previously overlooked morphotypes of nine-banded armadillo, especially a very distinctive unit circumscribed to the Guiana Shield. **Discussion.** As our results are congruent with recent molecular data and analyses of the structure of paranasal sinuses, we propose that *D. novemcinctus* should be regarded either as a polytypic species (with three to four subspecies) or as a complex of several distinct species.

1 **Beyond the carapace: skull shape variation and morphological systematics of**  
2 **long-nosed armadillos (genus *Dasypus*).**

3

4 Lionel Hautier<sup>1,2</sup>, Guillaume Billet<sup>3</sup>, Benoit de Thoisy<sup>4,5</sup>, and Frédéric Delsuc<sup>1</sup>

5

6 <sup>1</sup>Institut des Sciences de l'Evolution, UMR5554, CNRS, IRD, EPHE, Université de Montpellier,  
7 Montpellier, France.

8 <sup>2</sup>Mammal Section, Life Sciences, Vertebrate Division, The Natural History Museum, Cromwell  
9 Road, London SW7 5BD, UK.

10 <sup>3</sup>Sorbonne Universités, CR2P, UMR 7207, CNRS, Université Paris 6, Muséum National  
11 d'Histoire Naturelle, Paris, France.

12 <sup>4</sup>Institut Pasteur de la Guyane, Cayenne, French Guiana.

13 <sup>5</sup>Kwata NGO, BP 972, Cayenne, French Guiana.

14

15

16 **Corresponding Author**

17 Lionel Hautier

18 Email address: [lionel.hautier@umontpellier.fr](mailto:lionel.hautier@umontpellier.fr).

19 **Abstract**

20 **Background.** The systematics of long-nosed armadillos (genus *Dasypus*) has been mainly based  
21 on a handful of external morphological characters and classical measurements. Here, we studied  
22 the pattern of morphological variation in the skull of long-nosed armadillos species, with a focus  
23 on the systematics of the widely distributed nine-banded armadillo (*D. novemcinctus*).

24 **Methods.** We present the first exhaustive 3D comparison of the skull morphology within the  
25 genus *Dasypus*, based on  $\mu$ CT-scans. We used geometric morphometric approaches to explore  
26 the patterns of the intra- and interspecific morphological variation of the skull with regard to  
27 several factors such as taxonomy, geography, allometry, and sexual dimorphism.

28 **Results.** We show that the shape and size of the skull vary greatly between *Dasypus* species,  
29 with *D. pilosus* representing a clear outlier compared to other long-nosed armadillos. The study  
30 of the cranial intraspecific variation in *D. novemcinctus* evidences clear links to the geographic  
31 distribution and argues in favour of a revision of past taxonomic delimitations. Our detailed  
32 morphometric comparisons detected previously overlooked morphotypes of nine-banded  
33 armadillos, especially a very distinctive unit circumscribed to the Guiana Shield.

34 **Discussion.** As our results are congruent with recent molecular data and analyses of the structure  
35 of paranasal sinuses, we propose that *D. novemcinctus* should be regarded either as a polytypic  
36 species (with three to four subspecies) or as a complex of several distinct species.

## 37 Introduction

38 With their Pan-American distribution, long-nosed armadillos (genus *Dasybus*) constitute an  
39 understudied model for Neotropical biogeography. They are the most taxonomically diverse and  
40 widespread extant xenarthrans. The genus *Dasybus* traditionally comprises seven extant species  
41 (*D. novemcinctus*, *D. hybridus*, *D. septemcinctus*, *D. kappleri*, *D. pilosus*, *D. mazzai*, and *D.*  
42 *sabanicola*; Wetzel, 1985; Wilson & Reeder, 2005; Feijo & Cordeiro-Estrela, 2014) and two  
43 extinct ones (*D. bellus* and *D. punctatus*; Castro et al., 2013; Castro, 2015). In spite of being one  
44 of the earliest diverging cingulate lineages (Gaudin & Wible, 2006; Delsuc et al., 2012; Gibb et  
45 al., 2016), the dasypodid early evolutionary history remains poorly known (Castro, 2015). Only  
46 three extinct genera were recognized among the Dasypodini: *Anadasypus* from the middle  
47 Miocene of Colombia and late Miocene of Ecuador (Carlini, Vizcaíno & Scillato-Yané, 1997;  
48 Carlini et al., 2013), *Pliodasybus* from the late Pliocene of Venezuela (Castro et al., 2014), and  
49 *Propraopus* from the middle Pleistocene–early Holocene of South America (Castro et al.,  
50 2013a).

51       Aside the widespread nine-banded armadillo (*D. novemcinctus*), all extant long-nosed  
52 armadillos are restricted to South America. Some species are sympatric in certain areas resulting  
53 in competition and possibly supporting divergent behaviours and morphologies. The nine-banded  
54 armadillo is likely to be the most abundant armadillo in tropical forests (Wetzel & Mondolfi,  
55 1979; Loughry & McDonough, 1998) and has the widest distribution of all extant xenarthran  
56 species. Its distribution is thought to cover much of South and Central America and parts of  
57 North America and ranges from the south-east United States to North western Argentina and  
58 Uruguay (McBee & Baker, 1982). The species ability to disperse quickly, as well as its  
59 opportunistic and generalist mode of life, could partly explain this large distribution (Smith &

60 Doughty, 1984; Loughry & Mcdonough, 1998) marked by its rapid historical expansion into the  
61 United States (Taulman & Robbins, 2014). Such a wide geographical distribution, combined  
62 with early-recognized morphological variations (Peters, 1864; Gray, 1873; Allen, 1911;  
63 Lönnberg, 1913; Russell, 1953), raise the possibility that major taxonomic subgroups have been  
64 overlooked, be it at the subspecific or even specific level.

65         As its vernacular name implies, the genus *Dasypus* is characterized by a long, slender  
66 rostrum, which represents at least more than 55% of the length of the head (Gardner, 2008). The  
67 different species are usually distinguished by body and cranial measurements, colour differences,  
68 and morphological features of the carapace such as the number of movable bands and scutes  
69 across the body and the number and shape of osteodermal foramina (Feijo & Cordeiro-Estrela,  
70 2016). The carapace is a hallmark of armadillos, and constitutes such a unique feature for  
71 mammals that it has dominated the attention of early and modern anatomists and, as a result,  
72 partly jeopardized the classification of the group. Its morphology, chiefly the number of movable  
73 bands, has been intensively, if not abusively, used in systematic studies. However, even in the  
74 so-called nine-banded armadillo, the number of movable bands can vary from 7 to 10 (Wetzel &  
75 Mondolfi, 1979). Yet early on, in his *Systema Naturae* (ed. 10, p. 51), (Linnaeus, 1758) casted  
76 doubt on the use of the number of movable bands as a criterion to distinguish *Dasypus* species  
77 (*i.e.*, *D. septemcinctus* from *D. novemcinctus*). Since then, a number of authors have raised the  
78 question whether such external features could be confidently used for systematic purposes.  
79 Wetzel and Mondolfi (1979) argued that “although many scientific names of armadillos are  
80 based on the number of movable bands, it is proposed here that for vernacular names we  
81 discontinue using this variable characteristic and base names upon unique or more consistent  
82 features”. In the early 20<sup>th</sup> century, Hamlett (1939) made similar observations when focusing on

83 the nine-banded armadillo; he considered as impossible to recognize external variations at a  
84 subspecific level and concluded that “cranial characters appear to offer the only promise for  
85 subspecific analysis of the species” (Hamlett 1939:335). We decided to take up and further  
86 discuss Hamlett’s idea since no large review of the dasypodine cranial variation has been  
87 undertaken to date.

88 This study aims to further elucidate the pattern of morphological variation seen in the  
89 skull of long-nosed armadillos, with a focus on the nine-banded armadillo. Geometric  
90 morphometric data were collected for most *Dasypus* species using  $\mu$ CT-scans. The main  
91 questions asked in the present study were whether different patterns of variation in skull shape  
92 can be characterized among and within long-nosed armadillo species, and if those patterns could  
93 be linked to factors such as taxonomy, geographical distribution, skull size, or sexual  
94 dimorphism. Our ultimate goals are to reconstruct the details of the biogeographic distribution of  
95 the widespread nine-banded armadillo at the continental scale and to lay the path for a new  
96 integrative taxonomy of long-nosed armadillos. A greater understanding of the morphological  
97 diversity and patterns of evolution for long-nosed armadillos is timely to effectively conserve  
98 these species and will also serve to deepen our knowledge of their peculiar evolution and biology  
99 (Loughry & Mcdonough, 2013).

100

## 101 **Materials & Methods**

### 102 ***Biological samples***

103 The material studied came from the collections of the *Muséum national d’Histoire naturelle* in  
104 Paris (MNHN, collections *Zoologie et Anatomie comparée, Mammifères et Oiseaux*), the Natural  
105 History Museum in London (BMNH), the Naturalis Biodiversity Center in Leiden (NBC), the

106 Royal Ontario Museum in Toronto (ROM), the Louisiana State University in Bâton-Rouge  
107 (LSU), the American Museum of Natural History in New York (AMNH), the National Museum  
108 of Natural History in Washington (USNM), the *Instituto de Pesquisas Científicas e Tecnológicas*  
109 *do Estado do Amapá* in Macapá (IEPA), and the *Muséum d'Histoire naturelle* in Geneva, the  
110 KWATA association in Cayenne, and the Personal collection of Pierre Charles-Dominique. We  
111 analysed 128 skulls belonging to five *Dasypus* species (see Table S1 for a complete list of  
112 specimens): *D. novemcinctus*, *D. hybridus*, *D. septemcinctus*, *D. kappleri*, and *D. pilosus* (no  
113 data was available for *D. yepesi*, and *D. sabanicola*). With these data we performed a  
114 preliminary assessment of the average amounts of cranial variation at the specific level among  
115 different populations of *D. novemcinctus* from French Guiana, Guyana, Suriname, Ecuador,  
116 Brazil, Venezuela, Colombia, Costa Rica, Belize, Bolivia, Argentina, Paraguay, Uruguay,  
117 Panama, Nicaragua, Honduras, Guatemala, Mexico, Peru, and USA (Table S1). Juvenile,  
118 subadult, and adult specimens were considered in order to take into account the effect of age,  
119 size and differential growth on the dataset. Several studies (Hensel, 1872; Russell, 1953;  
120 Ciancio, Castro & Asher, 2012) showed that long-nosed armadillos possess tooth replacement, as  
121 typical for mammals, and that the eruption of permanent teeth occurs relatively late, as observed  
122 in afrotherians (Asher & Lehmann, 2008). Accordingly, we used eruption of the teeth, suture  
123 closure, and size as criteria to identify adult specimens in our dataset.

124

### 125 ***Geometric morphometric methods***

126 Due to the limitations of the classical qualitative descriptive approach, geometric morphometrics  
127 represents a good complementary technique by which to examine intraspecific shape variation.  
128 Digital data of all specimens were acquired using X-ray micro-computed tomography ( $\mu$ CT) at



129 the University of Montpellier (France), at the Natural History Museum (London, UK), and at the  
130 AST-RX platform MNHN (Paris, France). Three-dimensional reconstruction and visualization of  
131 the skulls were performed using stacks of digital  $\mu$ CT images with AVIZO v. 6.1.1 software  
132 (Visualization Sciences Group 2009). The mandibles and crania of armadillos were quantified  
133 with 10 and 84 anatomical landmarks respectively (Fig. 1 and Tables 1 and 2) using ISE-  
134 MeshTools (version 1.3.1; Lebrun, 2014). These landmarks were inspired by previous studies  
135 performed on different mammalian taxa (Hautier, Lebrun & Cox, 2012; Hautier et al., 2014).  
136 Considering the tendency to the reduction of the number of teeth in *Dasyopus* specimens (Allen,  
137 1911), which often lack the last dental locus and thus produce an artificial shortening of the  
138 entire tooth row, we decided to place a landmark after the seventh teeth and not at the end of the  
139 tooth row as it is usually the norm. Since skulls were often incomplete, the number of landmarks  
140 was adjusted to account for the maximal morphological variation in a maximum number of  
141 individuals; this number was then different whether we performed analyses considering all  
142 *Dasyopus* species (10 and 84 landmarks for the mandible and the cranium respectively) or only *D.*  
143 *novemcinctus* (10 and 82 landmarks for the mandible and the cranium respectively).

144 All configurations (sets of landmarks) were superimposed using the Procrustes method of  
145 generalized leastsquares superimposition (GLS scaled, translated, and rotated configurations so  
146 that the intralandmark distances were minimized) following the methods of Rohlf (1999) and  
147 Bookstein (1991). Subsequently, mandibular and cranial forms of each specimen were  
148 represented by centroid size  $S$ , and by multidimensional shape vector  $v$  in linearized Procrustes  
149 shape space. Shape variability of the skull and the mandible was analysed by Principal  
150 Component Analysis (PCA) of shape (Dryden & Mardia, 1998). Analysis and visualization of  
151 patterns of shape variation were performed with the interactive software package

152 MORPHOTOOLS (Specht, 2007; Specht, Lebrun & Zollikofer, 2007; Lebrun, 2008; Lebrun et  
153 al., 2010).

154 To account for the potentially confounding effects of size allometry on shape, size-  
155 corrected shapes were obtained as follows. In a first step, allometric patterns were obtained via  
156 regression of Procrustes coordinates against the logarithm of centroid size, yielding an allometric  
157 shape vector (ASV), which characterizes cranial allometric patterns. In a second step, regressions  
158 of Procrustes coordinates against the logarithm of centroid size were computed for all species,  
159 yielding species-specific allometric shape vectors (ASVs). The ASVs represent directions in  
160 shape space that characterize species-specific allometric patterns of shape variation. A common  
161 allometric shape vector (ASVc), obtained as the mean of all the ASVs, provided a direction in  
162 shape space that minimizes potential divergence in mandibular allometric patterns across species  
163 (see Lebrun et al., 2010 for further details concerning this methodology). PCres corresponds to  
164 principal components of a PCA performed on shape data corrected for allometry. The same  
165 analyses have been performed at the intraspecific level and regressions were then computed  
166 between the Procrustes coordinates and the logarithm of centroid size for all subgroups (defined  
167 at a country level).

168 Multivariate analyses of variance (MANOVA) were performed on the principal component  
169 scores of mandibular and cranial mean shapes (35 first PCs, i.e. 90% of the variance) in order to  
170 assess the effects of different factors on mandibular and cranial shape variation: clades (species),  
171 sex, and geographic distribution (countries). MANOVAs were performed with Past 2.06 (Hammer,  
172 Harper & Ryan, 2001). Linear discriminant analyses (LDA) of shape coordinates were  
173 performed on the same number of PCs to assess a potential discrimination of skull morphology  
174 in relation to phylogeny (*i.e.*, species) and geography (*i.e.*, countries). When a group included

175 only one individual, this specimen was integrated into the dataset as ungrouped cases. A skull  
176 from Panama (USNM 171052) was not complete enough to be considered in these analyses. We  
177 then decided to perform similar analyses with a reduced set of landmarks (71 landmarks on the  
178 cranium) to enable morphological comparisons with other specimens.

179

### 180 *Linear measurements*

181 Several linear measurements of the skull of *Dasypus* were calculated directly on 3D coordinates  
182 of landmarks (Fig. 2). These measurements were used to compare our results with traditional  
183 methods of species delineation.

184

## 185 **Results**

### 186 *Interspecific variation of skull shape among long-nosed armadillos*

187 A MANOVA performed on the first 35 PCs (i.e. 90% of the variance) indicates a significant  
188 morphological differentiation of the mandibles and crania relative to species delimitations  
189 (mandible Wilks' lambda=0.01164, F=4.903, p<0.001; cranium Wilks' lambda=0.0005897,  
190 F=11, p<0.001). A multivariate regression of the shape component on size, estimated by the  
191 logarithm of centroid size, was highly significant for the skull (mandible Wilks' lambda=0.2709,  
192 F=6.637, p<0.001; cranium Wilks' lambda=0.0632, F=30.92, p<0.001). When looking at the  
193 allometric shape vectors obtained with the centroid size, we found that size explains 18.99% and  
194 25.58% of the variation in the whole mandibular and cranial data sets respectively (S2A and  
195 S3A).

196 Morphological differences occur among the mandibles of the five species of *Dasypus*  
197 (Fig. 3A). The first two principal components (24.73 % and 16.48% of total shape variation)

198 weakly discriminates *D. pilosus* (negative values) from *D. kappleri* (positive values) while all  
199 specimens of *D. novemcinctus*, *D. hybridus*, and *D. septemcinctus* sit in the middle of the graph.  
200 These axes separate mandibles having a slender horizontal ramus with an elongated anterior part  
201 (located in front of the tooth row) and a short ascending ramus with a short coronoid process  
202 anteriorly positioned and vertically oriented from mandibles showing a high horizontal ramus  
203 with a short anterior part and a long ascending ramus with an elongated and distally oriented  
204 coronoid process. Mandibles of different size are poorly discriminated along the first principal  
205 component (Fig. 3B). Once the effect of allometry is removed (S4), no clear morphological  
206 differentiation is visible along PCres1. All taxa but *D. pilosus* lay in the positive values of  
207 PCres2 therefore the variation in this component is mostly restricted to this latter species.

208         The interspecific differences in the cranium of *Dasypus* are apparent in the morphospace  
209 defined by the first two principal components. Except for *D. hybridus* and *D. septemcinctus*, all  
210 species are well discriminated in the morphospace defined by the two first principal components  
211 (Fig. 4A), which explain 28,4% and 14,6% of the variance respectively. The first principal  
212 component unequivocally discriminates *D. hybridus* and *D. septemcinctus* from other species,  
213 and negatively correlates with a shortened rostrum and enlarged basicranium and braincase (Fig.  
214 4A). *D. pilosus* individuals are well discriminated on the second principal component. On PC2  
215 (Fig. 4A), the crania of *D. pilosus* appear narrower with a long snout and smaller braincase  
216 (positive values) whereas the crania of *D. novemcinctus*, *D. kappleri*, *D. hybridus*, and *D.*  
217 *septemcinctus* are wider with a shorter snout and relatively small braincase (negative values). A  
218 regression of the first principal component on the logarithm of the centroid size (Fig. 4B) clearly  
219 shows that the five species show different size ranges. The biggest crania are long and display  
220 longer and wider snout; whereas the smallest crania are short and wide posteriorly and

221 characterized by a short snout. *D. pilosus* clearly remains an outlier once the size effect is  
222 removed (S5), while the other species appear less differentiated in the cranium morphospace.  
223 The specific differentiation was checked by performing a discriminant analysis and using a  
224 classification phase. The classification methods recovered 100% correct classification of  
225 specimens.

226 We also performed the same analyses this time including juvenile specimens (S6) but  
227 excluding *D. pilosus* since it represents a clear outlier in the morphospace. All juvenile  
228 specimens of *D. novemcinctus* tend to congregate in the negative values of the PC1 and then  
229 appear more similar in shape to *D. septemcinctus* and *D. hybridus* than the adults. All juveniles  
230 of *D. novemcinctus* and *D. septemcinctus* are located in more negative values of PC1 and more  
231 positive values of PC2 relative to the adult individuals of their own species. Such a distribution  
232 in the morphospace defined by PC1-2 suggests similar ontogenetic trajectories for the two  
233 species.

234

### 235 ***Intraspecific variation of skull shape in nine-banded armadillos***

236 In specimens for which sex was available (22 females and 32 males for the mandible; 19 females  
237 and 34 males for the cranium), a MANOVA shows that there is no sexual dimorphism present in  
238 the cranial data (Wilks' lambda=0.2429, F=1.514, p=0.182), so sex is unlikely to be responsible  
239 for the variation observed in the cranium of *D. novemcinctus*, while it might partly be for the  
240 mandible (Wilks' lambda=0.2292, F=2.579, p=0.0110). A multivariate regression of the shape  
241 component on size was highly significant (mandible, Wilks' lambda=0.3468, F=3.454, p <0.001;  
242 cranium, Wilks' lambda=0.1447, F=8.446, p <0.001). When looking at the allometric shape  
243 vectors obtained with the centroid size (S2B and S3B), we found that size explains 14.14% and

244 14.32% of the variation in the whole mandibular and cranial data sets respectively. Shape data  
245 corrected for allometry are presented in S7 and S8.

246 A weak intraspecific differentiation (per country) is noticeable on the mandibular  
247 morphology (mandible, Wilks' lambda=0.0001404, F=1.523, p <0.001; Fig. 5A). The first  
248 principal component (9.87% of total shape variation) weakly discriminates specimens from  
249 Brazil, Bolivia, Paraguay, Uruguay (positive values) from other specimens (negative values).  
250 This axis separates mandibles characterized by robust and short horizontal ramus and long  
251 ascending ramus with a high coronoid, low condylar, and poorly individualized angular  
252 processes from mandibles with slender and elongated horizontal ramus and short ascending  
253 ramus with low coronoid, high condylar, and well individualized angular processes (Fig. 5A). In  
254 terms of shape variation, PC2 (4.745% of total shape variation) separates mandibles that show  
255 elongated anterior part of the horizontal ramus, short tooth row, high and distally oriented  
256 coronoid process from mandibles having reduced anterior part of the horizontal ramus, an  
257 elongated tooth row, and low coronoid process. We observed even less differentiation with shape  
258 data corrected for allometry (S7), which indicates that some specimens differ significantly in  
259 size. This is confirmed by a regression of the first principal component on the logarithm of the  
260 centroid size (Fig. 5B) that shows that the specimens from Brazil, Uruguay, Paraguay, Bolivia,  
261 Peru, Ecuador, Costa Rica, and Colombia are usually smaller.

262 A MANOVA was also used to explore if the cranial variation matches the geographical  
263 distributions of *D. novemcinctus* (Wilks' lambda=2.97x10<sup>-6</sup>, F=2.157, p <0.001). When looking  
264 at the cranial morphological variation according to geographic origin (*i.e.*, countries) (Fig. 6),  
265 several trends can be observed. PC1, accounting for 22.7% variation, demonstrates a change in  
266 how domed the dorsal surface of the skull is and positively correlates with an increase in snout

267 length, a decrease in braincase size, jugals more extended dorsoventrally, and shorter pterygoid  
268 processes (Fig. 6A). Specific clusters are recognizable on the first principal component with  
269 specimens from Brazil, Paraguay, Venezuela (USNM 406700 from Clarines area, North),  
270 Ecuador (BMNH-14-4-25-86 from Gualaquiza, South East), Colombia (AMNH 136252 from  
271 Villavicencio area, Centre), Peru, Bolivia, Paraguay, and Uruguay that congregate in the  
272 negative values whereas all other specimens lay in the positive values. PC2 is responsible for  
273 8.6% of the variance, and describes variation in the size of the posterior part of the rostrum; it  
274 also displays variation in length of the posterior part of the palate with an anterior border of the  
275 palatine that is well behind the posterior end of the tooth row in positive values. This axis mainly  
276 separates specimens from USA, Mexico, Belize, Honduras, Guatemala, and Nicaragua (negative  
277 values) from other specimens (positive values). We observed less specific differentiation with  
278 shape data corrected for allometry (S8), which shows that the different geographical subgroups  
279 differ significantly in size. This is confirmed by a regression of the first principal component to  
280 the logarithm of the centroid size (Fig. 7).

281         A Linear Discriminant Analysis (LDA) of shape coordinates was performed in order to  
282 take into account the entire morphological variation (*i.e.*, 35 first PCs that represent 90.6% of the  
283 variance) and to maximize discrimination among specimens belonging to different countries.  
284 Only countries for which we had several specimens could be considered here. Three main  
285 regional groups were clearly recovered by the analysis (Fig. 8A): a Northern morphotype, a  
286 Southern morphotype, and a group circumscribed to the Guiana Shield (GS). The first group  
287 from North and Central America includes specimens from the US, Mexico, Guatemala, and  
288 Belize. The South American group gathers specimens from Brazil, Uruguay, Bolivia, Peru,  
289 Colombia, and Venezuela. Finally, specimens from French Guiana, Suriname, and Guyana



290 congregate in a last distinctive group. Some specimens from Colombia, Venezuela, and Ecuador  
291 do not gather with any of those groups and sit in the middle of the graph defined by the first two  
292 discriminant axes; these specimens are however well discriminated on the third and fourth  
293 discriminant axes (Fig. 8B) and might constitute a fourth individualized regional group among  
294 *D. novemcinctus*, called hereafter the Central morphotype.

295         The discriminant model used to separate the regional groups was checked using a  
296 classification phase and then used on under-sampled countries (*i.e.*, when  $n=1$ ) to assess their  
297 affiliation to one of the four abovementioned groups. This classification showed 95% correct  
298 classification of specimens (S9). Most regional misclassifications were with specimens coming  
299 from the limit of the distribution range of the groups. Two Brazilian specimens from Amapa are  
300 put together with the Guianan specimens (S9) and confirmed previous results from the PCA  
301 where these two specimens clearly depart from the rest of the Brazilian specimens (Fig. 6A).  
302 Three specimens from Venezuela (USNM 406700 from Clarines area, North), Ecuador (BMNH-  
303 14-4-25-86 from Gualaquiza, South East), and Colombia (AMNH 136252 from Villavicencio  
304 area, Centre) were *a posteriori* classified as close to the Southern morphotype. All these  
305 specimens were collected East of the Andes (Fig. 9) and grouped with Brazilian specimens in the  
306 PCA analyses. Concerning the countries for which only one specimen was available, the  
307 classification analyses gave congruent results with the grouping proposed by the principal  
308 component analysis: specimens from Paraguay and Peru were classified as being part of the  
309 Southern morphotype while specimens from Nicaragua, Honduras, and Costa Rica were  
310 classified as grouping with the Northern morphotype (S9). Using a reduced set of landmarks, the  
311 specimen from Panama was attributed to the Central morphotype. When performing these  
312 classification methods using the four groups as factors (*i.e.*, Northern, Central, Southern, and



313 Guianan morphotypes; see S10), instead of countries, we retrieved 100% correct classification of  
314 specimens.

315 We performed very similar analyses (PCA and LDA, see S11) using linear cranial  
316 measurements traditionally used in systematic studies. In all cases, these analyses failed to  
317 retrieve a clear-cut discrimination between the four groups defined above.

318

## 319 **Discussion**

### 320 *Morphological variation of skull among Dasypus species*

321 Skull ratios are commonly used to compare *Dasypus* species, especially the length of the palate  
322 to length of skull (PL/CNL) and length of rostrum to length of skull (RL adj./CNL) (Wetzel,  
323 1985). Three subgenera are commonly recognized on this basis: *Cryptophractus* (including *D.*  
324 *pilosus*), *Hyperoambon* (including *D. kappleri*), and *Dasypus* (including all remaining species)  
325 (Wetzel & Mondolfi, 1979). Our results are largely consistent with findings from previous  
326 studies regarding existing differences between *Dasypus* species. Allometry substantially explains  
327 cranial differences, with the exception of *D. pilosus* that does not follow the main dasypodine  
328 allometric trend (Figs. 3 and 4). The hairy long-nosed armadillo clearly departs from the other  
329 four *Dasypus* species in being mainly characterized by a lengthening of the snout and mandible  
330 and a small development of the braincase and basicranium. All these characteristics were linked  
331 to their unique diet, which might predominantly include ants and termites (Castro et al., 2015).  
332 Considering these distinctive morphological features and a specific structure of its osteoderms,  
333 Castro et al. (2015) recently proposed to include *D. pilosus* in a different genus, i.e.  
334 *Cryptophractus*. However, recent molecular results (Gibb et al., 2016) did not support such a  
335 taxonomic reassessment and argued for the conservation of the hairy long-nosed armadillo in the

336 genus *Dasypus*. *D. pilosus* thus likely represents a case of rapid acquisition (*i.e.*, 2.8 Ma as  
337 estimated by Gibb et al., 2016) of distinctive morphological traits in line with the shift to a  
338 divergent behaviour and ecology.

339 Both molecular and morphological data suggested that *D. kappleri* is broadly separated  
340 from the other *Dasypus* species (Wetzel & Mondolfi, 1979; Gibb et al., 2016). Mitogenomic data  
341 clearly identified *D. kappleri* as the sister group to all other *Dasypus* species from which it  
342 diverged more than 12 million years ago (Gibb et al., 2016) and suggested to place it in the  
343 distinct genus *Hyperoambon*, as originally proposed by Wetzel and Mondolfi (1979). We  
344 retrieved a significant morphological differentiation with all the specimens of *D. kappleri*  
345 congregating in the morphospace and being much larger than the other species. However, the  
346 cranial morphology of *D. kappleri* still remains very close to that of *D. novemcinctus* when  
347 compared to that of *D. septemcinctus*, *D. hybridus*, and *D. pilosus* (Fig. 4). Recently, Feijo and  
348 Cordeiro-Estrela (2016) proposed to recognize three species within *D. kappleri* based on  
349 morphological differences of the skull and carapace: *D. kappleri* distributed in the Guiana shield;  
350 *D. pastasae* occurring from the eastern Andes of Peru, Ecuador, Colombia, and Venezuela south  
351 of the Orinoco River into the western Brazilian Amazon; and finally *D. beniensis* that occurs in  
352 the lowlands of the Amazonian Brazil and Bolivia to the south of the Madre de Dios, Madeira,  
353 and lower Amazon rivers. We only had access to a limited number of specimens but did not  
354 retrieve such a clear geographical segregation in shape (S12A), while we observed a mild  
355 differentiation in size with the Guianan *D. kappleri* being usually bigger (S12B).

356 Wetzel and Mondolfi (1979:47) placed *D. septemcinctus*, *D. hybridus*, and *D. sabanicola*  
357 in the same subgenus together with *D. novemcinctus*. We observed that *D. hybridus* and *D.*  
358 *septemcinctus* group together in the morphospace, but are largely separated from *D.*

359 *novemcinctus*. These two species are usually distinguished by external features, *D. hybridus*  
360 showing shorter ears and a longer tail than *D. septemcinctus* (Hamlett, 1939; Wetzel &  
361 Mondolfi, 1979). Our morphometrical results showed that *D. hybridus* and *D. septemcinctus*  
362 display very similar cranial and mandibular morphologies; they also display several cranial  
363 characteristics in common with juvenile specimens of *D. novemcinctus*. Such morphological  
364 similarities echo recent molecular findings (Gibb et al., 2016) that showed that mitogenomic  
365 sequences of *D. hybridus* are almost identical to those of an Argentinian *D. septemcinctus*  
366 (99.3% identity). The two species were considered as valid based on cranial and body  
367 measurements (Hamlett, 1939; Wetzel, 1985) despite the fact that they display many external  
368 resemblances and have very close geographical distribution. A recent study of their internal  
369 cranial sinuses also failed to provide diagnostic characters for the distinction of these two genera  
370 (Billet et al., unpublished data). Our samples were very limited for both *D. hybridus* (n=4) and  
371 *D. septemcinctus* (n=3), but additional samplings will undoubtedly help to define the systematic  
372 status of the two species.

373 We did not have access to the two most recently recognized *Dasypus* species: the  
374 Yunga's lesser long-nosed armadillo *D. mazzai* (Yepes, 1933), and the northern long-nosed  
375 armadillo *D. sabanicola* (Mondolfi, 1967). The validity of the former was and is still hotly  
376 debated (Wetzel & Mondolfi, 1979; Vizcaíno, 1995; Gardner, 2008; Feijo & Cordeiro-Estrela,  
377 2014), while the specific status of the latter also remains controversial (Wetzel & Mondolfi,  
378 1979; Wetzel, 1985). Cranial morphometric data might provide insightful arguments to discuss  
379 the systematic status of the two species.

380

381 ***Morphological systematics and skull shape variation in Dasypus***

382 Relative skull shape has previously been examined for systematics purposes in the genus  
383 *Dasypus* but never with a focus on patterns of intraspecific variation. Hamlett (1939) casted  
384 doubt on the possibility to identify different subgroups within *D. novemcinctus*, while early  
385 workers had already recognized several, either at a specific or at a subspecific level. Peters  
386 (1864) described *Dasypus fenestratus* from Costa Rica based on the position of the small and  
387 numerous major palatine foramina, some of which are connected to the incisive foramina  
388 through a groove, between (not in front of) the anterior teeth, its medially shorter palatine bones,  
389 the position of the palatine suture posterior to the end of the tooth row, the position of the  
390 lacrimal foramen closer to the orbital rim, as well as one character on the extent of the pelvic  
391 shield of the carapace. Gray (1873) tentatively recognized as many as seven species of nine-  
392 banded armadillos in South and Central Americas, among which five of them were new: *Tatusia*  
393 (= *Dasypus*) *granadiana*, *T. leptorhynchus*, *T. brevirostris*, *T. leptocephala*, and *T. boliviensis*. He  
394 also followed Peters (1864) and recognized *T. mexicana* (a variety of *D. novemcinctus* in Peters  
395 1864), but decided to ignore *T. fenestratus*. Both Peters (1864) and Gray (1873) used a very  
396 small number of specimens and Gray (1873) distinguished all these species based mainly on the  
397 morphology of the lacrimal bones and minute morphological variation of the head scutes. Allen  
398 (1911) later considered *D. fenestratus* and *D. mexicanus* as synonym taxa of subspecific level  
399 (*D. novemcinctus fenestratus* Peters). He also described *D. novemcinctus hoplites* from Grenada,  
400 a subspecies that he considered to be distinctly characterized by a shorter tooth row due to the  
401 absence of the last tooth locus.

402 From the inspection of a series of specimens from Panama, Costa Rica, and Yucatan,  
403 Allen (1911) also distinguished a Central American morphotype. Compared to Brazilian  
404 specimens, Allen's Central American armadillo is characterized by short palatine bones that do

405 not reach the level of the most posterior teeth, an obvious inflation of the maxillary region  
406 located in front of the lacrimal bone, as well as a lateral margin of the skull that is largely convex  
407 at the level of the second or third tooth in ventral view. Based on size differences, Haggmann  
408 (1908) described the subspecies *D. n. mexiana*, which he thought was restricted to a small area  
409 close to the mouth of the Amazon River. Lönnberg (1913) defined *D. n. aequatorialis* from  
410 Ecuador, which McBee and Baker (1982) later proposed to consider as a probable synonym to *T.*  
411 *granadiana* Gray 1873. His comparisons were based on morphological characteristics of the  
412 carapace, *D. n. aequatorialis* showing differences of the occipital portion of the frontal shield as  
413 well as different proportions of the scales of the shoulder and pelvic shields. Later on, Russel  
414 (1953) proposed to recognize two subspecies in Mexico: *D. n. davis* in north-western part of  
415 Mexico and *D. n. mexicanus* present in most of the country. Even if it is close morphologically to  
416 *D. n. mexicanus*, *D. n. davis* is much smaller in size and displays a few distinctive features such  
417 as small maxillary teeth, a narrow mandible with an angular process posteriorly projected, and  
418 differences in suture closure patterns and shape with for instance the parietal-frontal sutures that  
419 lies well behind the posterior process of the zygomatic arch (Russell, 1953). Most of these early  
420 descriptions, be them at a specific and subspecific level, were based on subtle morphological  
421 differences and no proper quantification of the skull variation was undertaken up to now.

422 Our statistical analysis of the skull shape demonstrated that *D. novemcinctus* exhibits a  
423 significant level of intraspecific variation, with several clearly identified groups within the nine-  
424 banded armadillo. While male nine-banded armadillos tend to be slightly larger than females  
425 (McBee & Baker, 1982), our multivariate analyses first suggest the absence of sexual  
426 dimorphism in the cranium and a slight sexual dimorphism in the mandible. We also show that  
427 allometry is likely to explain a substantial part of the observed morphological variation,

428 including geographically. This echoes early findings by Wetzel and Mondolfi (1979) who  
429 already pointed out size gradients between different populations of *D. novemcinctus*. Our  
430 morphometric analysis successfully retrieved such a geographical differentiation, both in size  
431 and shape. Interestingly, our geometric morphometric analyses permitted to define four discrete  
432 phenotypic units. These units display very different cranial characters and occupy very distinct  
433 geographical distributions, which are in essence allopatric.

434         Specimens from Brazil, Uruguay, Paraguay, Bolivia, Peru, and from regions of Ecuador,  
435 Colombia, and Venezuela located east of the Andes make up most of one group and show a very  
436 stable pattern of variation (Fig. 9); they are on average smaller than the three remaining groups.  
437 Skulls of this Southern morphotype are clearly distinct by showing smaller and flatter skulls with  
438 short frontal sinuses, a narrow snout with short premaxillar bones, a narrow interorbital width, a  
439 long and slender jugal part of the zygomatic arch, longer pterygoid processes, and a basicranium  
440 aligned with the palate in lateral view (Fig. 6). We found no sign of morphological  
441 differentiation of specimens from the mouth of the Amazon River, as implied by the proposed  
442 recognition of the subspecies *D. n. mexiana* (Hagmann, 1908). The area covered by the  
443 specimens attributed to this morphological unit fully encompasses that of the Amazon basin and  
444 seemed to be delimited by the Andes on the western side. As a matter of fact, the single  
445 Ecuadorian specimen coming from the eastern side of the Andes appeared to be distinct from  
446 most other Ecuadorian specimens, but morphologically close to Brazilian and Bolivian  
447 specimens. The same holds true for the Peruvian, Colombian, and Venezuelan specimens  
448 collected east of the Andes. The distribution of this group is reminiscent of that of the subspecies  
449 *D. novemcinctus novemcinctus* Linnaeus, except for the Guiana Shield area (Gardner, 2008). It  
450 also recalls a similar lineage molecularly identified (Arteaga et al., unpublished data) and the

451 Southern morphotype evidenced by the analysis of paranasal spaces (Billet et al., unpublished  
452 data). Unfortunately the type specimen of *D. novemcinctus*; which is supposedly housed in the  
453 Swedish Museum of Natural History in Stockholm (Lönnerberg, 1913), could not be included in  
454 our analyses. The type locality of *Dasyurus novemcinctus* Linnaeus is “America meridionali” and  
455 is generally thought to be from the eastern coast of Brazil (Allen, 1911).

456         The next differentiated group is represented by individuals originating from the Guiana  
457 shield region including French Guiana, Guyana, Suriname, and Amapa in Brazil (Fig. 9). All the  
458 specimens belonging to this Guianan morphotype display large dome-shaped skulls that share  
459 distinctive morphological features including long frontal sinuses, a wide snout with long  
460 premaxillar bones, a large interorbital width, large lacrimal bones, a short and massive jugal part  
461 of the zygomatic arch, an anterior border of the palatine located well behind the posterior end of  
462 the tooth row, shorter pterygoid processes, and a basicranium situated above the palatal plane  
463 (Fig. 6). Studies of paranasal sinuses agree with the distinctness of this group and show that the  
464 dome-shaped frontal region of Guianan nine-banded armadillos is occupied by a  
465 characteristically inflated pair of frontal sinuses that extend posteriorly to the fronto-parietal  
466 suture (Billet et al., unpublished data). No subspecies has ever been recognized or proposed in this  
467 part of South America, and such a clear-cut morphological divergence of Guianan specimens of  
468 *D. novemcinctus* is here proposed for the first time. These morphometric findings corroborate  
469 recent molecular studies, which showed that specimens from French Guiana are very distant  
470 from the US populations (Huchon et al., 1999) and represent a distinct branch in the dasypodine  
471 mitogenomic tree (Gibb et al., 2016; Arteaga et al., submitted).

472         The distribution of the third recognized morphological group is more limited. It is  
473 distributed from the western Andes of Ecuador, Colombia, Panama, and Venezuela to Costa Rica



474 (Fig. 9). This Central morphotype is characterized by high and short skulls having moderately  
475 developed frontal sinuses, long premaxillar bones, a narrow interorbital width (larger than  
476 Southern specimens but narrower than Guianan specimens), a massive anterior part of the  
477 zygomatic arch that is much larger than the posterior part, a short and high jugal part of the  
478 zygomatic arch that is largely convex ventrally, an anterior border of the palatine located well  
479 behind the posterior end of the tooth row, shorter pterygoid processes, and a basicranium well  
480 above the palatal plan (Fig. 6). This distribution roughly corresponds to the combined ranges of  
481 two previously described subspecies: *D. n. fenestratus* (Peters, 1864) and *D. n. aequatorialis*  
482 (Lönnberg, 1913). These close morphological resemblances suggest that these subspecies might  
483 be synonym taxa. However, we could not fully test this hypothesis since we had only access to  
484 one specimen from West of the Andes in Peru, Ecuador and southern Bolivia. Studies on the  
485 paranasal spaces (Billet et al., unpublished data) failed to recognize such a group, and instead  
486 gathered some specimens from these regions with specimens from North and Central America,  
487 while others (from the western parts of Colombia, Venezuela and from Panama) were judged  
488 impossible to be confidently referred to a given frontal sinus morphotype. In contrast, molecular  
489 studies recovered a lineage similar to the group recognized here distributing from the Northern  
490 Andes and Central America but expanding to western Mexico (Arteaga et al., unpublished data).

491 The last distinct morphotype occurs from Nicaragua to the Southern part of the US (Fig.  
492 9). The range of this Northern morphotype spans the proposed distribution areas of the  
493 subspecies *D. n. mexicanus* and *D. n. davisii*, as well as the northernmost part of the distribution  
494 range of *D. n. fenestratus*. All the skulls from this area display moderately developed frontal  
495 sinuses convergent toward the midline, long premaxillar bones, a narrow interorbital width  
496 (larger than Southern specimens but narrower than Guianan specimens), a long and slender jugal



497 part of the zygomatic arch that is largely convex ventrally, an anterior border of the palatine  
498 located at the level of the posterior end of the tooth row, shorter pterygoid processes, and a  
499 basicranium slightly above the palatal plan (Fig. 6). Contrary to Russel (1953), we did not find  
500 major morphological cranial differences between north-western and eastern Mexican  
501 populations. Our results thus cast doubts on the validity of the subspecies *D. n. davisi*. The  
502 morphological homogeneity in this group is also at odds with the presence of two mitochondrial  
503 lineages in Mexico (Arteaga et al., 2012, submitted) but is coherent with the presence of nuclear  
504 gene flow between them (Arteaga et al., 2011). Within this Northern group, the invasive US  
505 armadillo population derived from two geographical sources: one from Mexico and one from  
506 south-central Florida where captive animals were presumably released (Loughry & McDonough,  
507 2013). For a long time, the exact origin of the Floridian introduced population remained  
508 uncertain. All the US specimens used in our analyses were proved to belong to the same  
509 Northern morphotype. Echoing the results obtained on six microsatellite loci described by  
510 Loughry et al. (2009), we interpret our findings as indicative of a close relationship between the  
511 two US populations. The recognition of this Northern unit with individuals ranging from Central  
512 to Northern America is also in agreement with their distinctive pattern of paranasal sinuses  
513 (Billet et al., unpublished data).

514         The newly recognized subgroups within *D. novemcinctus* prompt questions about the role  
515 of ecological factors likely to have influenced their morphological differentiation. Morphological  
516 variation in skull morphology as a result of ecological factors has been studied in a number of  
517 species over recent years (*e.g.*, Caumul and Polly, 2005; Wroe and Milne, 2007; Hautier et al.,  
518 2012). Factors such as temperature, diet and competition may cause phenotypic variation and are  
519 likely to explain some morphological differences between the identified groups. These ecological

520 factors vary in relation to geography, and differences in geographical distribution can drive  
521 selection for different phenotypes, which may eventually lead to distinctive populations or even  
522 new species. Since the four *D. novemcinctus* subgroups are not sympatric in most of their  
523 respective natural range, we can hypothesize that environment and/or genetic drift, but not  
524 competition, may be responsible for some of the observed intraspecific variation. The Northern  
525 Andes constitute a clear geographical barrier, which limited contacts between Northern/Central  
526 and Southern populations, and thus has likely played a major role in shaping the morphological  
527 differentiation of the long-nosed armadillos. This biogeographical barrier seems to have played a  
528 significant role in xenarthrans since it also marks the separation between the two living species  
529 of tamanduas with *Tamandua mexicana* in the north and *T. tetradactyla* in the south (Superina,  
530 Miranda & Abba, 2010), also within naked-tailed armadillos with *Cabassous centralis* in the  
531 north and *C. unicinctus* in the south (Abba & Superina, 2010).

532         The geographical distribution of the divergent populations of *D. novemcinctus* recalls the  
533 pattern of morphological differentiation recently proposed for the greater long-nosed armadillo  
534 (*D. kappleri*), especially for the Guianan specimens (Feijo & Cordeiro-Estrela, 2016). However,  
535 in the nine-banded armadillo, we did not find a clear morphological differentiation within the  
536 Amazonian basin as defined on the opposite banks of the Madeira-Madre de Dios rivers (Feijo &  
537 Cordeiro-Estrela, 2016), which separate *D. pastasae* from *D. beniensis*. Given the extent of  
538 morphological variation reported within *D. kappleri*, Feijo and Cordeiro-Estrela (2016)  
539 interpreted their findings as indicative of the fact that this species complex diverged earlier than  
540 other *Dasypus* species, which would allow them to accumulate more differences. Such a  
541 hypothesis seems difficult to conceive in view of the substantial morphological variation  
542 observed among different populations of *D. novemcinctus*, which have diverged more recently

543 (3.7 Ma, Gibb et al., 2016). Feijo and Cordeiro-Estrela (2016) also proposed that such  
544 cumulative differences may result from strong environmental selective pressures. The newly  
545 discovered morphological diversity within *D. kappleri* and *D. novemcinctus* is likely to represent  
546 parallel cases of allopatric differentiation in response to diverging environmental pressures. In  
547 both cases, only the future collecting of large-scale genomic nuclear data will allow testing these  
548 taxonomic proposals based on morphological data.

549

## 550 **Conclusions**

551 Intraspecific variations can be the result of adaptation to varying local environmental conditions.  
552 We showed that morphometrical comparisons enable detection of previously overlooked  
553 morphotypes and yield new insights into factors likely to explain differences between  
554 populations inhabiting different areas. Our study of the intraspecific variation of the skull in *D.*  
555 *novemcinctus* evidences clear links to the geographic distribution and allows a revision of past  
556 taxonomic delimitations. Based on the cranial differences observed, we consider that *D.*  
557 *novemcinctus* should be regarded either as a polytypic species (with three to four subspecies) or  
558 as a complex of several species. In particular, a new unit of nine-banded armadillos from the  
559 Guiana Shield could be detected, which is in agreement with most recent investigations of  
560 molecular data and internal anatomy (Arteaga et al., unpublished data; Billet et al., unpublished  
561 data). The discovery of divergent populations within *D. novemcinctus* has implications for  
562 conservation of the species. In some areas, human activities have led to habitat degradation and  
563 fragmentation (Zimbres et al., 2013) or even to habitat loss. These divergent populations may be  
564 under threat and may require conservation measures, or at least a close re-examination of their  
565 conservation status. If we were to consider them as separate management unit and not as a single

566 species with a large distribution, the threat of endangerment to *D. novemcinctus* would need re-  
567 evaluation since it is currently classified globally as ‘Least Concern’ by the IUCN (Loughry,  
568 McDonough & Abba, 2014). In addition, our results demonstrate that specimens of *D.*  
569 *novemcinctus* should be chosen with caution when making anatomical comparisons or  
570 performing cladistic analyses (*e.g.*, Castro et al., 2015); their geographical distribution should be  
571 at least specified in all cases. This morphological investigation needs to be extended to the other  
572 parts of the body, the carapace in particular. The cranial differences detected among the defined  
573 groups might be linked to previously detected differences in the number and shape of scutes on  
574 the head shield (*e.g.*, Lönnberg, 1913). Geometric morphometric data holds out the possibility of  
575 studying effectively covariation patterns between osteological parts and features of the carapace.  
576 Given the quality of the cingulate fossil record, using geometric morphometric methods seems  
577 equally conceivable on extinct forms and might also provide fruitful ways to interpret past  
578 morphological diversity.

579

## 580 **Acknowledgements**

581 We are grateful to Christiane Denys, Violaine Nicolas, and Géraldine Véron, (Muséum National  
582 d’Histoire Naturelle, Paris), Roberto Portela Miguez, Louise Tomsett and Laura Balcells (British  
583 Museum of Natural History, London), Eileen Westwig (American Museum of Natural History,  
584 New-York), Burton Lim (Royal Ontario Museum, Toronto), Nicole Edmison and Chris Helgen  
585 (National Museum of Natural History, Washington), Jake Esselstyn (Louisiana State University,  
586 Baton-Rouge), Manuel Ruedi (*Muséum d’Histoire naturelle*, Geneva), Claudia Regina da Silva  
587 (*Instituto de Pesquisas Científicas e Tecnológicas do Estado do Amapá*, Macapá), Steven van  
588 der Mije (Naturalis Biodiversity Center, Leiden), François Cazeflis and Suzanne Jiquel (Institut

589 des Sciences de l'Evolution, Montpellier), Lucile Dudoignon (KWATA association), Dominique  
590 Charles (CNRS), Maria-Clara Arteaga, Maria Nazareth da Silva (*Instituto de Pesquisas*  
591 *Científicas e Tecnológicas do Estado do Amapá*) for access to comparative material. We thank  
592 Clara Belfiore for her help in the data acquisition. R. Lebrun (Institut des Sciences de  
593 l'Evolution, Montpellier), Farah Ahmed (British Museum of Natural History, London), Miguel  
594 García-Sanz and Florent Goussard (Platform AST-RX MNHN) generously provided help and  
595 advice on the acquisition of CT scans. Some of the experiments were performed using the  $\mu$ -CT  
596 facilities of the Montpellier Rio Imaging (MRI) platform and of the LabEx CeMEB. This is  
597 contribution ISEM 2017-XXX of the Institut des Sciences de l'Evolution.

598

599

## 600 **Funding**

601 This work has benefited from an "Investissements d'Avenir" grant managed by Agence Nationale  
602 de la Recherche, France (CEBA, ref. ANR-10-LABX-25-01). This research received support  
603 from the Synthesys Project (<http://synthesys3.myspecies.info/>), which is financed by the  
604 European Community Research Infrastructure Action under the FP7.

605

606

## 607 **Grant Disclosures**

608 The following grant information was disclosed by the authors:

609 Agence Nationale de la Recherche: contract ANR-10-LABX-25-01.

610

611

612 **Competing Interests**

613 The authors declare no competing interests.

614

615

616 **Author Contributions**

617 • Lionel Hautier conceived and designed the experiments, contributed materials, performed the  
618 experiments, analysed the data, wrote the paper.

619 • Guillaume Billet conceived and designed the experiments, contributed materials.

620 • Benoit de Thoisy contributed materials.

621 • Frédéric Delsuc conceived and designed the experiments, contributed materials.

622 • All authors read, discussed, corrected, and approved the final version of the paper.

623

624

625 **Data Deposition**

626 The following information was supplied regarding the deposition of related data:

627 Dryad, <http://dx.doi.org/xxxxx>.

628 **References**

- 629 Abba AM., Superina M. 2010. The 2009/2010 armadillo red list assessment. *Edentata* 11:135–  
630 184.
- 631 Allen G. 1911. Mammals of the west indies. *Bulletin of the useum of Comparative Zoology*  
632 54:175–263.
- 633 Arteaga MC., McCormack JE., Eguiarte LE., Medellín RA. 2011. Genetic admixture in  
634 multidimensional environmental space: asymmetrical niche similarity promotes gene flow  
635 in armadillos (*Dasypus novemcinctus*). *Evolution* 65:2470–2480.
- 636 Arteaga MC., Piñero D., Eguiarte LE., Gasca J., Medellín R. 2012. Genetic structure and  
637 diversity of the nine-banded armadillo in Mexico. *Journal of Mammalogy* 93:547–559.
- 638 Asher RJ., Lehmann T. 2008. Dental eruption in afrotherian mammals. *BMC biology* 6:14. DOI:  
639 10.1186/1741-7007-6-14.
- 640 Bookstein F. 1991. *Morphometric tools for landmark data. Geometry and biology*. Cambridge:  
641 Cambridge University Press.
- 642 Carlini A a., Castro MC., Madden RH., Scillato-Yané GJ. 2013. A new species of Dasypodidae  
643 (Xenarthra: Cingulata) from the late Miocene of northwestern South America: implications  
644 in the Dasypodini phylogeny and diversity. *Historical Biology*:37–41. DOI:  
645 10.1080/08912963.2013.840832.
- 646 Carlini A., Vizcaíno S., Scillato-Yané G. 1997. Armored xenarthrans: a unique taxonomic and  
647 ecologic assemblage. In: Kay R, Madden R, Cifelli R, Flynn J. eds. *Vertebrate paleontology*  
648 *in the Neotropics. The Miocene Fauna of La Venta, Colombia*. Washington/London:  
649 Smithsonian Institution Press, 213–226.
- 650 Castro MC. 2015. Sistemática y evolución de los armadillos Dasypodini (Xenarthra, Cingulata,

- 651 Dasypodidae). *Revista del Museo de La Plata* 15:1–50.
- 652 Castro MC., Avilla LS., Freitas ML., Carlini AA. 2013a. The armadillo *Propraopus sulcatus*  
653 (Mammalia: Xenarthra) from the late Quaternary of northern Brazil and a revised synonymy  
654 with *Propraopus grandis*. *Quaternary International* 317:80–87. DOI:  
655 10.1016/j.quaint.2013.04.032.
- 656 Castro MC., Carlini A a., Sánchez R., Sánchez-Villagra MR. 2014. A new Dasypodini armadillo  
657 (Xenarthra: Cingulata) from San Gregorio Formation, Pliocene of Venezuela: Affinities and  
658 biogeographic interpretations. *Naturwissenschaften* 101:77–86. DOI: 10.1007/s00114-013-  
659 1131-5.
- 660 Castro MC., Ciancio MR., Pacheco V., Salas-Gismondi RM., Bostelmann JE., Carlini AA. 2015.  
661 Reassessment of the hairy long-nosed armadillo “*Dasypus*”*pilosus* (Xenarthra,  
662 Dasypodidae) and revalidation of the genus *Cryptophractus* Fitzinger, 1856. *Zootaxa*  
663 3947:30–48. DOI: 10.11646/zootaxa.3947.1.2.
- 664 Castro MC., Ribeiro AM., Ferigolo J., Langer MC. 2013b. Redescription of *Dasypus punctatus*  
665 Lund, 1840 and considerations on the genus *Propraopus* Ameghino, 1881. *Journal of*  
666 *Vertebrate Paleontology* 33:434–447. DOI: 10.1080/02724634.2013.729961.
- 667 Caumul R., Polly P. 2005. Phylogenetic and environmental components of morphological  
668 variation: skull, mandible, and molar shape in marmots (*Marmota*, Rodentia). *Evolution*  
669 59:2460–2472.
- 670 Ciancio MR., Castro MC., Asher RJ. 2012. Evolutionary implications of dental eruption in  
671 *Dasypus* (Xenarthra). *Journal of Mammalian Evolution* 19:1–8. DOI: 10.1007/s10914-011-  
672 9177-7.
- 673 Delsuc F., Superina M., Tilak M., Douzery EJP., Hassanin A. 2012. Molecular Phylogenetics



- 674 and Evolution Molecular phylogenetics unveils the ancient evolutionary origins of the  
675 enigmatic fairy armadillos. *Molecular Phylogenetics and Evolution* 62:673–680. DOI:  
676 10.1016/j.ympev.2011.11.008.
- 677 Dryden I., Mardia K. 1998. *Statistical shape analysis*. Chichester: John Wiley & Sons.
- 678 Feijo A., Cordeiro-Estrela P. 2014. The correct name of the endemic *Dasyopus* (Cingulata:  
679 Dasypodidae) from northwestern Argentina. *Zootaxa* 3887:88–94. DOI:  
680 10.11646/zootaxa.3887.1.6.
- 681 Feijo A., Cordeiro-Estrela P. 2016. Taxonomic revision of the *Dasyopus kappleri* complex, with  
682 revalidations of *Dasyopus pastasae* (Thomas, 1901) and *Dasyopus beniensis* Lönnberg, 1942  
683 (Cingulata, Dasypodidae). *Zootaxa* 4170:271–297. DOI: 10.11646/zootaxa.4170.2.3.
- 684 Gardner AF. 2008. *Mammals of South America Volume 1 Marsupials, Xenarthrans, Shrews, and*  
685 *Bats*. Chicago and London: The University of Chicago Press.
- 686 Gaudin TJ., Wible JR. 2006. The Phylogeny of Living and Extinct Armadillos (Mammalia,  
687 Xenarthra, Cingulata): A Craniodental Analysis. In: Carrano M, Gaudin TJ, Blob R, Wible  
688 JR eds. *Amniote Paleobiology: Perspectives on the Evolution of Mammals, Birds and*  
689 *Reptiles*. Chicago: The University of Chicago Press, 153–198.
- 690 Gibb GC., Condamine FL., Kuch M., Enk J., Moraes-Barros N., Superina M., Poinar HN.,  
691 Delsuc F. 2016. Shotgun mitogenomics provides a reference phylogenetic framework and  
692 timescale for living xenarthrans. *Molecular Biology and Evolution* 33:621–642. DOI:  
693 10.1093/molbev/msv250.
- 694 Gray J. 1873. *Handlist of the edentate, thick-skinned, and ruminant mammals of the British*  
695 *Museum*. London: British Museum of Natural History.
- 696 Haggmann G. 1908. Die Landsäugetiere der insel Mexiana. Als Beispiel der Einwirkung der

- 697 isolation auf die umbildung der arten. *Arch. Rass.-Gesell.-Biol. München* 5:1–32.
- 698 Hamlett G. 1939. Identity of *Dasypus septemcinctus* Linnaeus with notes on some related  
699 species. *Journal of Mammalogy* 20:328–336.
- 700 Hammer Ø., Harper D., Ryan P. 2001. PAST: paleontological statistics software package for  
701 education and data analysis. *Paeontologica Electronica* 4:9.
- 702 Hautier L., Billet G., Eastwood B., Lane J. 2014. Patterns of Morphological Variation of Extant  
703 Sloth Skulls and their Implication for Future Conservation Efforts. *Anatomical Record*  
704 297:979–1008. DOI: 10.1002/ar.22916.
- 705 Hautier L., Lebrun R., Cox PG. 2012. Patterns of covariation in the masticatory apparatus of  
706 hystricognathous rodents: implications for evolution and diversification. *Journal of*  
707 *morphology* 273:1319–37. DOI: 10.1002/jmor.20061.
- 708 Hensel R. 1872. *Beiträge zur Kenntnis der Säugethiere Süd-Brasiliens*. Berlin: lis den  
709 Abhandlungen der Königl. Akademie der Wissenschaften.
- 710 Huchon D., Delsuc F., Catzeflis F., Douzery EJP. 1999. Armadillos exhibit less genetic  
711 polymorphism in North America than in South America: nuclear and mitochondrial data  
712 confirm founder effect in *Dasypus novemcinctus* (Xenarthra). *Molecular Ecology* 8:1743–  
713 1748.
- 714 Lebrun R. 2008. Evolution and development of the strepsirrhine primate skull. University  
715 Montpellier II and University of Zürich.
- 716 Lebrun R. 2014. ISE-MeshTools, a 3D interactive fossil reconstruction freeware. In: *12th Annual*  
717 *Meeting of EAVP*. Torino,.
- 718 Lebrun R., Ponce de León M., Tafforeau P., Zollikofer C. 2010. Deep evolutionary roots of  
719 strepsirrhine primate labyrinthine morphology. *Journal of Anatomy* 216:368–380.

- 720 Linnaeus C. 1758. *Systema Naturae, Ed; 10. L.* Uppsala: Salvii.
- 721 Lönnberg E. 1913. Mammals from Ecuador and related forms. *Arkiv för Zoologi* 8:1–36.
- 722 Loughry WJ., Mcdonough CM. 1998. Comparisons between nine-banded armadillo (*Dasyopus*  
723 *novemcinctus*) populations in brazil and the united States. *Revista de biologia tropical*  
724 46:1173–1183.
- 725 Loughry WJ., Mcdonough CM. 2013. *The nine-banded armadillo: a natural history.* Norman:  
726 University of Oklahoma Press.
- 727 Loughry J., McDonough C., Abba A. 2014. *Dasyopus novemcinctus.* *The IUCN Red List of*  
728 *Threatened Species* 2014:e.T6290A47440785.
- 729 Loughry WJ., Truman RW., McDonough CM., Tilak M-K., Garnier S., Delsuc F. 2009. Is  
730 leprosy spreading among nine-banded armadillos in the southeastern United States? *Journal*  
731 *of Wildlife Diseases* 45:144–152. DOI: 10.7589/0090-3558-45.1.144.
- 732 McBee K., Baker RJ. 1982. *Dasyopus novemcinctus.* *Mammalian Species* 162:1–9.
- 733 Mondolfi E. 1967. Descripción de un nuevo armadillo del género *Dasyopus* de Venezuela  
734 (Mammalia-Edentata). *Memorias de la Sociedad de Ciencias Naturales La Salle* 78:149–  
735 167.
- 736 Peters W. 1864. Über neue Arten de Saugethier-gattungen *Geomys*, *Haplodon* und *Dasyopus*.  
737 *Monatsbericht der Königlich- Preussischen Akademie der Wissenschaften zu Berlin*  
738 1865:177–181.
- 739 Rohlf F. 1999. Shape statistics: Procrustes superimpositions and tangent spaces. *Journal of*  
740 *Classification* 16:197–223.
- 741 Russell R. 1953. Description of a new armadillo (*Dasyopus novemcinctus*) from mexico with  
742 remarks on geographic variation of the species. *Proceedings of the Biological Society of*

- 743 *Washington* 66:21–26.
- 744 Smith L., Doughty R. 1984. The amazing armadillo: geography of a folk critter. In: Austin:  
745 University of Texas Press, 134.
- 746 Specht M. 2007. Spherical surface parameterization and its application to geometric  
747 morphometric analysis of the braincase. University of Zürich Irchel.
- 748 Specht M., Lebrun R., Zollikofer C. 2007. Visualizing shape transformation between  
749 chimpanzee and human braincases. *The Visual Computer* 23:743–751.
- 750 Superina M., Miranda FR., Abba AM. 2010. The 2010 anteater red list assessment. *Edentata*  
751 11:96–114.
- 752 Taulman JF., Robbins LW. 2014. Range expansion and distributional limits of the nine-banded  
753 armadillo in the United States: an update of Taulman & Robbins (1996). *Journal of*  
754 *Biogeography* 41:1626–1630.
- 755 Vizcaíno SF. 1995. Identificación específica de las "mulitas", género *Dasyopus* L. (Mammalia;  
756 Dasyopodidae); del noroeste argentino. Descripción de una nueva especie. *Mastozoología*  
757 *Neotropical* 2:5–13.
- 758 Wetzel R. 1985. Taxonomy and distribution of armadillos. In: *The Evolution and Ecology of*  
759 *Armadillos, Sloths, and Vermilinguas*. Washington DC: Smithsonian Institution Press, 23–  
760 46.
- 761 Wetzel R., Mondolfi E. 1979. The subgenera and species of long-nosed armadillos, genus  
762 *Dasyopus*. In: Eisenberg J ed. *Vertebrate Ecology in the Northern Neotropic*. Washington  
763 DC: Smithsonian Institution Press, 43–63.
- 764 Wilson D., Reeder D. 2005. *Mammal species of the world: a taxonomic and geographic*  
765 *reference. 3rd ed.* Baltimore: Johns Hopkins University Press.

766 Wroe S., Milne N. 2007. Convergence and remarkably consistent constraint in the evolution of  
767 carnivore skull shape. *Evolution* 61:1251–1260.

768 Yepes J. 1933. Una especie nueva de “mulita” (Dasypodinae) para el norte argentino. *Physis*  
769 11:225–232.

770 Zimbres B., Furtado MM., Jácomo, Anah T. A. Silveira L., Sollmann R., Tôrres NM., Machado  
771 RB., Marinho-Filho J. 2013. The impact of habitat fragmentation on the ecology of  
772 xenarthrans (Mammalia) in the Brazilian Cerrado. *Landscape Ecology* 28:259–269.

773

774

775

## 776 **Table legends**

777 **Table 1.** Definitions of the landmarks used on the mandible.

778

779 **Table 2.** Definitions of the landmarks used on the cranium. Landmarks indicated with a star  
780 were not used in the intraspecific comparisons.

781 **Figure Legends**

782

783 **Figure 1.** Landmarks digitized on the mandible and the skull. Dorsal (A), lateral (B), and ventral  
784 views of the cranium; medial (C) and lateral (D) views of the mandible.

785

786 **Figure 2.** Illustration of the skull linear measurements. In blue, traditional measurements used in  
787 Wetzel (1985). *Abbreviations:* LTC, length between the anterior tip of the nasal and the  
788 posteriormost point of the supraoccipital; LR, rostral length; IOB, interorbital breadth; ILFB,  
789 inter lacrimal foramina breadth; BB, distance between the left and right intersections between the  
790 frontal, parietal, and squamosal sutures; NB, nasal breadth; NL, nasal length; LCB, length  
791 between the anterior tip of the premaxillar and the condyles; TL, length of the tooth row; PB,  
792 palate breadth; BZP, distance between the infraorbital and the maxillary foramina; MB, inter-  
793 meatus breadth; OCB, breadth between the lateral border of the occipital condyle.

794

795 **Figure 3.** (A) Principal component analysis (PC1 vs PC2) and associate patterns of  
796 morphological transformation for the mandible of five *Dasypus* species. (B) Regression of the  
797 first principal component on the logarithm of the centroid size ( $R^2=0.23$ ;  $p<0.001$ ). *Symbols:*  
798 blue squares, *D. kappleri*; black crosses, *D. novemcinctus*; green triangles, *D. hybridus*; green  
799 diamonds, *D. septemcinctus*; red circles, *D. pilosus*.

800

801 **Figure 4.** (A) Principal component analysis (PC1 vs PC2) and associate patterns of  
802 morphological transformation for crania of five *Dasypus* species. (B) Regression of the first  
803 principal component on the logarithm of the centroid size ( $R^2=0.55$ ;  $p<0.001$ ). *Symbols:* blue

804 squares, *D. kappleri*; black crosses, *D. novemcinctus*; green triangles, *D. hybridus*; green  
805 diamonds, *D. septemcinctus*; red circles, *D. pilosus*.

806

807 **Figure 5.** (A) Principal component analysis (PC1 vs PC2) and associate patterns of  
808 morphological transformation for mandibles of *Dasypus novemcinctus*. (B) Regression of the  
809 first principal component on the logarithm of the centroid size ( $R^2=0,035$ ;  $p=0.03$ ). *Symbols*:  
810 green diamonds, Bolivia; green triangle, Brazil (solid green triangles are for specimens from  
811 Amapa); green circles, Paraguay; green crosses, Peru; green squares, Uruguay; green bars,  
812 Venezuela; blue diamonds, Belize; blue “plus”, Guatemala; blue bars, Honduras; Blue squares,  
813 Mexico; blue crosses, Nicaragua; blue triangles, USA; blue circles, Costa Rica; black triangles,  
814 Colombia; black crosses, Ecuador; black stars, Panama; orange squares, French Guiana; orange  
815 crosses, Guyana; orange circles, Suriname.

816

817 **Figure 6.** Principal component analysis (A, PC1 vs PC2; B, PC3 vs PC4) and associate patterns  
818 of morphological transformation for crania of *Dasypus novemcinctus*. *Symbols*: green diamonds,  
819 Bolivia; green triangle, Brazil (solid green triangles are for specimens from Amapa); green  
820 circles, Paraguay; green crosses, Peru; green squares, Uruguay; green bars, Venezuela; blue  
821 diamonds, Belize; blue “plus”, Guatemala; blue bars, Honduras; Blue squares, Mexico; blue  
822 crosses, Nicaragua; blue triangles, USA; blue circles, Costa Rica; black triangles, Colombia;  
823 black crosses, Ecuador; orange squares, French Guiana; orange crosses, Guyana; orange circles,  
824 Suriname.

825

826 **Figure 7.** Regression of the first cranial principal component (*Dasypus novemcinctus*) on the

827 logarithm of the centroid size ( $R^2=0.15$ ;  $p<0.001$ ). *Symbols*: green diamonds, Bolivia; green  
828 triangle, Brazil (solid green triangles are for specimens from Amapa); green circles, Paraguay;  
829 green crosses, Peru; green squares, Uruguay; green bars, Venezuela; blue diamonds, Belize; blue  
830 “plus”, Guatemala; blue bars, Honduras; Blue squares, Mexico; blue crosses, Nicaragua; blue  
831 triangles, USA; blue circles, Costa Rica; black triangles, Colombia; black crosses, Ecuador;  
832 orange squares, French Guiana; orange crosses, Guyana; orange circles, Suriname.

833

834 **Figure 8.** Linear Discriminant Analysis (LDA) performed on cranial shape coordinates of  
835 *Dasypus novemcinctus*. *Symbols*: green diamonds, Bolivia; green triangle, Brazil (solid green  
836 triangles are for specimens from Amapa); green circles, Paraguay; green crosses, Peru; green  
837 squares, Uruguay; green bars, Venezuela; blue diamonds, Belize; blue “plus”, Guatemala; blue  
838 bars, Honduras; Blue squares, Mexico; blue crosses, Nicaragua; blue triangles, USA; black  
839 triangles, Colombia; black circles, Costa Rica; black crosses, Ecuador; orange squares, French  
840 Guiana; orange crosses, Guyana; orange circles, Suriname.

841

842 **Figure 9.** Summary map showing the geographical distribution of nine-banded armadillo  
843 specimens investigated in this study and their attribution to one of the four main morphotypes  
844 defined in this study: black, Central group; blue, Northern group; green, Southern group; orange,  
845 Guianan group. Specimens lacking precise geographical information (other than country of  
846 origin) are indicated with a square.



847 **Supplemental Information**

848

849 **S1.** List of measured specimens (used for linear measurements and/or geometric morphometric  
850 analyses). *Abbreviations:* MNHN, *Muséum national d'Histoire naturelle* in Paris (collections  
851 *Zoologie et Anatomie comparée, Mammifères et Oiseaux*); BMNH, Natural History Museum in  
852 London; NBC, Naturalis Biodiversity Center in Leiden; ROM, Royal Ontario Museum in  
853 Toronto; LSU, Louisiana State University in Baton-Rouge; AMNH, American Museum of  
854 Natural History in New York; USNM, National Museum of Natural History in Washington;  
855 IEPA, *Instituto de Pesquisas Científicas e Tecnológicas do Estado do Amapá* in Macapá;  
856 MHNG, *Muséum d'Histoire naturelle* in Geneva; KWATA, KWATA association; and PCDPC,  
857 Personal collection of Pierre Charles-Dominique.

858

859 **S2.** Regression of the common allometric shape vector (ASVc) on the logarithm of the centroid  
860 size for mandibles of five *Dasypus* species (A,  $R^2=0.50$ ;  $p<0.001$ ) and *D. novemcinctus* (B,  
861  $R^2=0.34$ ;  $p<0.001$ ). Below, associate patterns of morphological transformation for mandibles  
862 with small (left) and large (right) centroid size. *Symbols:* same as in Figure 3 and 5.

863

864 **S3.** Regression of the common allometric shape vector (ASVc) on the logarithm of the centroid  
865 size for crania of five *Dasypus* species (A,  $R^2=0.72$ ;  $p<0.001$ ) and *D. novemcinctus* (B,  $R^2=0.48$ ;  
866  $p<0.001$ ). Below, associate patterns of morphological transformation for crania with small (left)  
867 and large (right) centroid size. *Symbols:* same as in Figure 3 and 5.

868

869 **S4.** Principal component analyses with shape data corrected for allometry (PCres1 vs PCres 2)

870 and associate patterns of morphological transformation for mandible of five *Dasyopus* species.

871 *Symbols*: blue squares, *D. kappleri*; black crosses, *D. novemcinctus*; green triangles, *D. hybridus*;

872 green diamonds, *D. septemcinctus*; red circles, *D. pilosus*.

873

874 **S5.** Principal component analyses with shape data corrected for allometry (PCres1 vs PCres 2)

875 and associate patterns of morphological transformation for crania of five *Dasyopus* species.

876 *Symbols*: blue squares, *D. kappleri*; black crosses, *D. novemcinctus*; green triangles, *D. hybridus*;

877 green diamonds, *D. septemcinctus*; red circles, *D. pilosus*.

878

879 **S6. (A)** Principal component analysis (PC1 vs PC2) and associate patterns of morphological

880 transformation for crania of five *Dasyopus* species, including juveniles (indicated with smaller

881 symbols) and excluding *D. pilosus*. **(B)** Regression of the first principal component on the

882 logarithm of the centroid size ( $R^2=0,63$ ;  $p<0.001$ ). *Symbols*: blue squares, *D. kappleri*; black

883 crosses, *D. novemcinctus*; green triangles, *D. hybridus*; green diamonds, *D. septemcinctus*.

884

885 **S7.** Principal component analyses with shape data corrected for allometry (PCres1 vs PCres 2)

886 and associate patterns of morphological transformation for mandibles of *Dasyopus specimens*.

887 *Symbols*: green diamonds, Bolivia; green triangle, Brazil (solid green triangles are for specimens

888 from Amapa); green circles, Paraguay; green crosses, Peru; green squares, Uruguay; green bars,

889 Venezuela; blue diamonds, Belize; blue “plus”, Guatemala; blue bars, Honduras; Blue squares,

890 Mexico; blue crosses, Nicaragua; blue triangles, USA; blue circles, Costa Rica; black triangles,

891 Colombia; black crosses, Ecuador; black stars, Panama; orange squares, French Guiana; orange

892 crosses, Guyana; orange circles, Suriname.

893

894 **S8.** Principal component analyses with shape data corrected for allometry (PCres1 vs PCres 2)

895 and associate patterns of morphological transformation for crania of *Dasypus specimens*.

896 *Symbols:* green diamonds, Bolivia; green triangle, Brazil (solid green triangles are for specimens

897 from Amapa); green circles, Paraguay; green crosses, Peru; green squares, Uruguay; green bars,

898 Venezuela; blue diamonds, Belize; blue “plus”, Guatemala; blue bars, Honduras; Blue squares,

899 Mexico; blue crosses, Nicaragua; blue triangles, USA; blue circles, Costa Rica; black triangles,

900 Colombia; black crosses, Ecuador; orange squares, French Guiana; orange crosses, Guyana;

901 orange circles, Suriname.

902

903 **S9.** Results of *a posteriori* classifications for the discriminant analysis performed on the cranial

904 shape coordinates of *Dasypus novemcinctus* using countries as factors. Specimens with a star (\*)

905 were integrated into the analyses as ungrouped cases.

906

907 **S10.** Results of *a posteriori* classifications for the discriminant analysis performed on the cranial

908 shape coordinates of *Dasypus novemcinctus* using the four subgroups (*i.e.*, Northern, Central,

909 Southern, and Guianan morphotypes) as factors. Specimens with a star (\*) were integrated into

910 the analyses as ungrouped cases.

911

912 **S11. (A)** Principal component analysis (PC1 vs PC2) and associate patterns of morphological

913 transformation for crania of *Dasypus kappleri*. **(B)** Regression of the first principal component

914 on the logarithm of the centroid size ( $R^2=0.40$ ;  $p<0.001$ ). *Symbols:* green crosses, Peru; green

915 bars, Venezuela; black triangles, Colombia; black crosses, Ecuador; orange squares, French

916 Guiana; orange crosses, Guyana; orange circles, Suriname.

# Figure 1

## Figure 1

Landmarks digitized on the mandible and the skull. Dorsal (A), lateral (B), and ventral views of the cranium; medial (C) and lateral (D) views of the mandible.

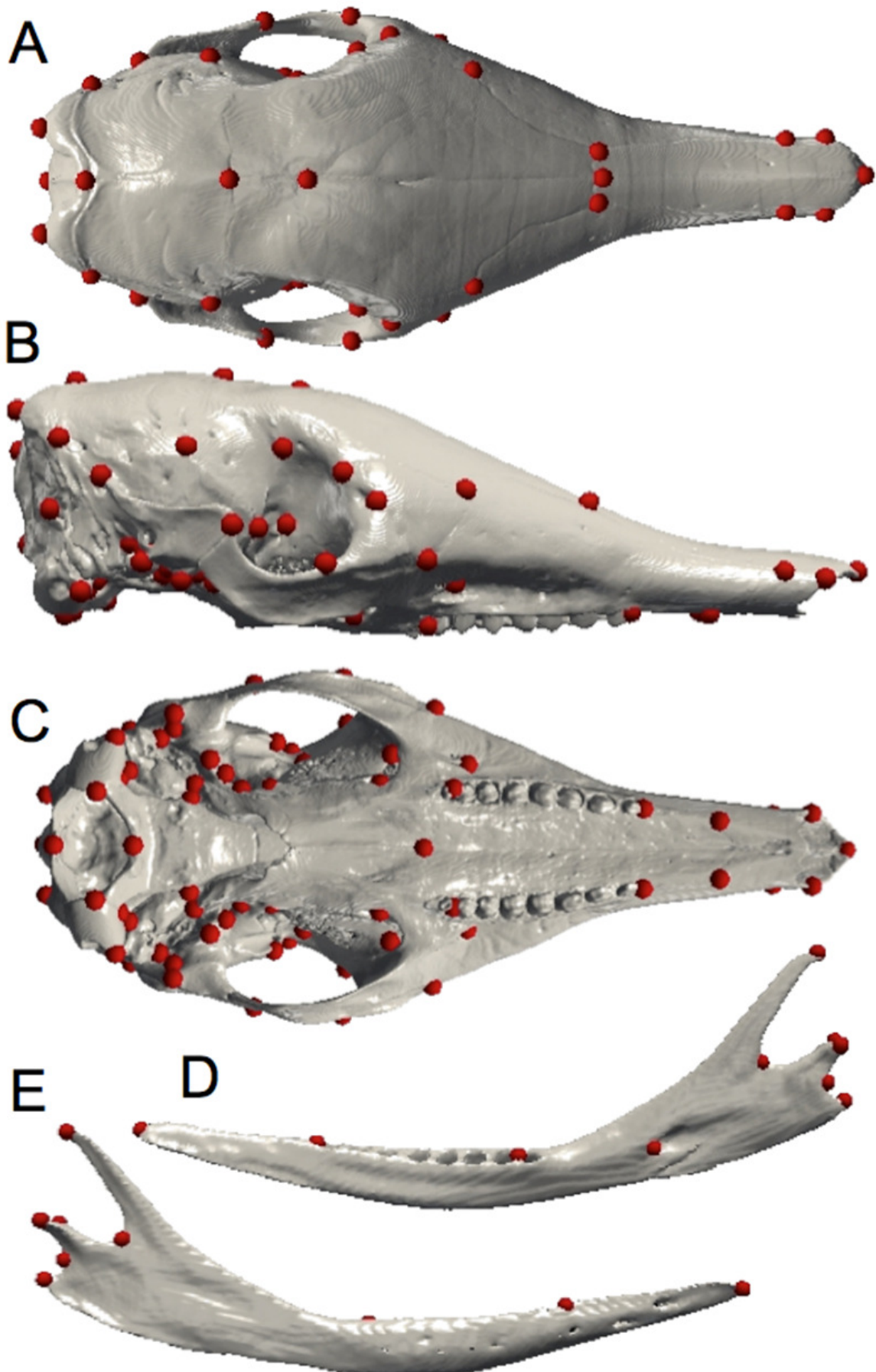


## Figure 2

### Figure 2

Illustration of the skull linear measurements. In blue, traditional measurements used in Wetzel (1985) . *Abbreviations:* LTC, length between the anterior tip of the nasal and the posteriormost point of the supraoccipital; LR, rostral length; IOB, interorbital breadth; ILFB, inter lacrimal foramina breadth; BB, distance between the left and right intersections between the frontal, parietal, and squamosal sutures; NB, nasal breadth; NL, nasal length; LCB, length between the anterior tip of the premaxillar and the condyles; TL, length of the tooth row; PB, palate breadth; BZP, distance between the infraorbital and the maxillary foramina; MB, inter-meatus breadth; OCB, breadth between the lateral border of the occipital condyle.

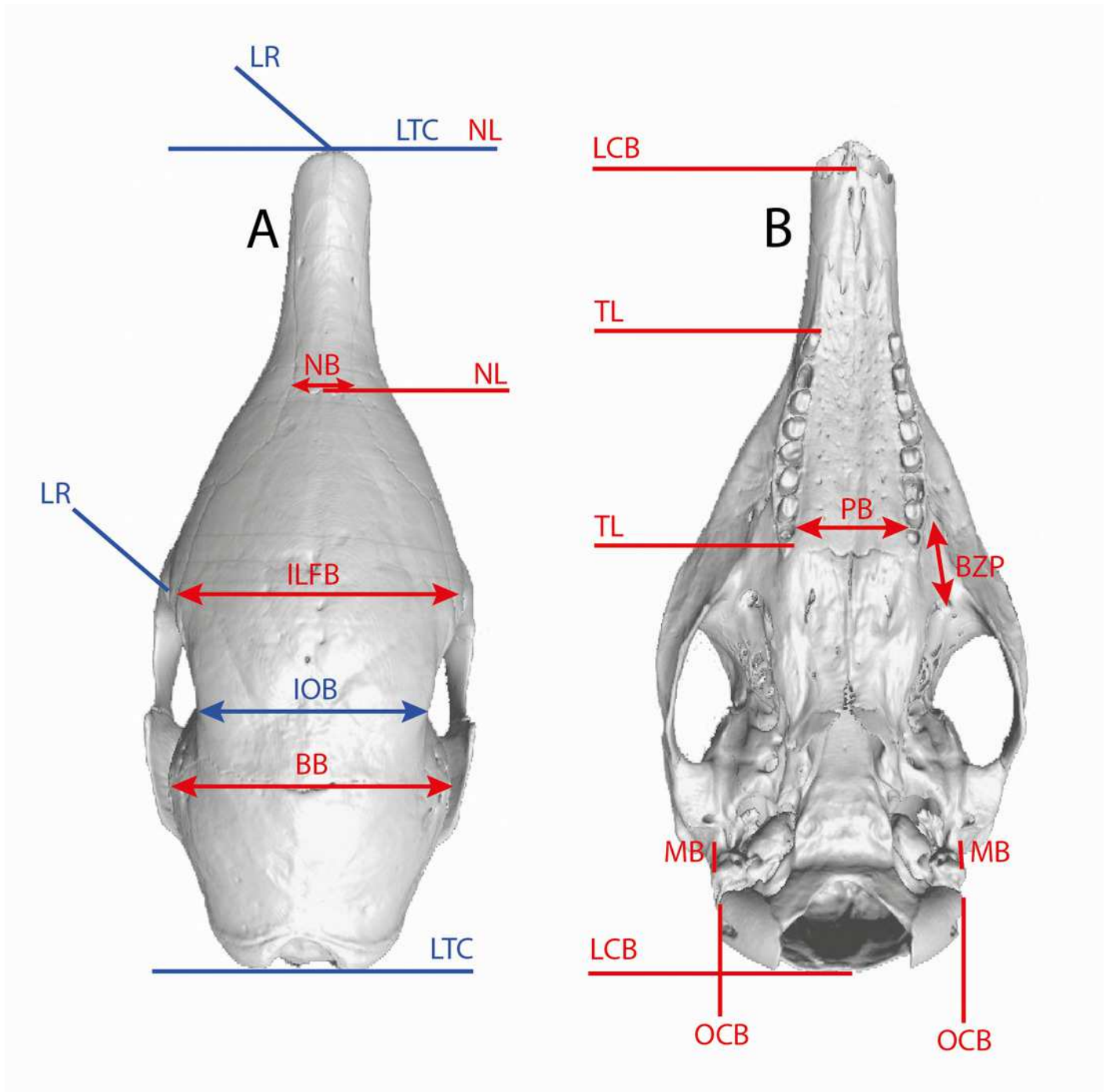




# Figure 3

Figure 3

(A) Principal component analysis (PC1 vs PC2) and associate patterns of morphological transformation for the mandible of five *Dasypus* species. (B) Regression of the first principal component on the logarithm of the centroid size ( $R^2=0.23$ ;  $p<0.001$ ). Symbols: blue squares, *D. kappleri*; black crosses, *D. novemcinctus*; green triangles, *D. hybridus*; green diamonds, *D. septemcinctus*; red circles, *D. pilosus*.

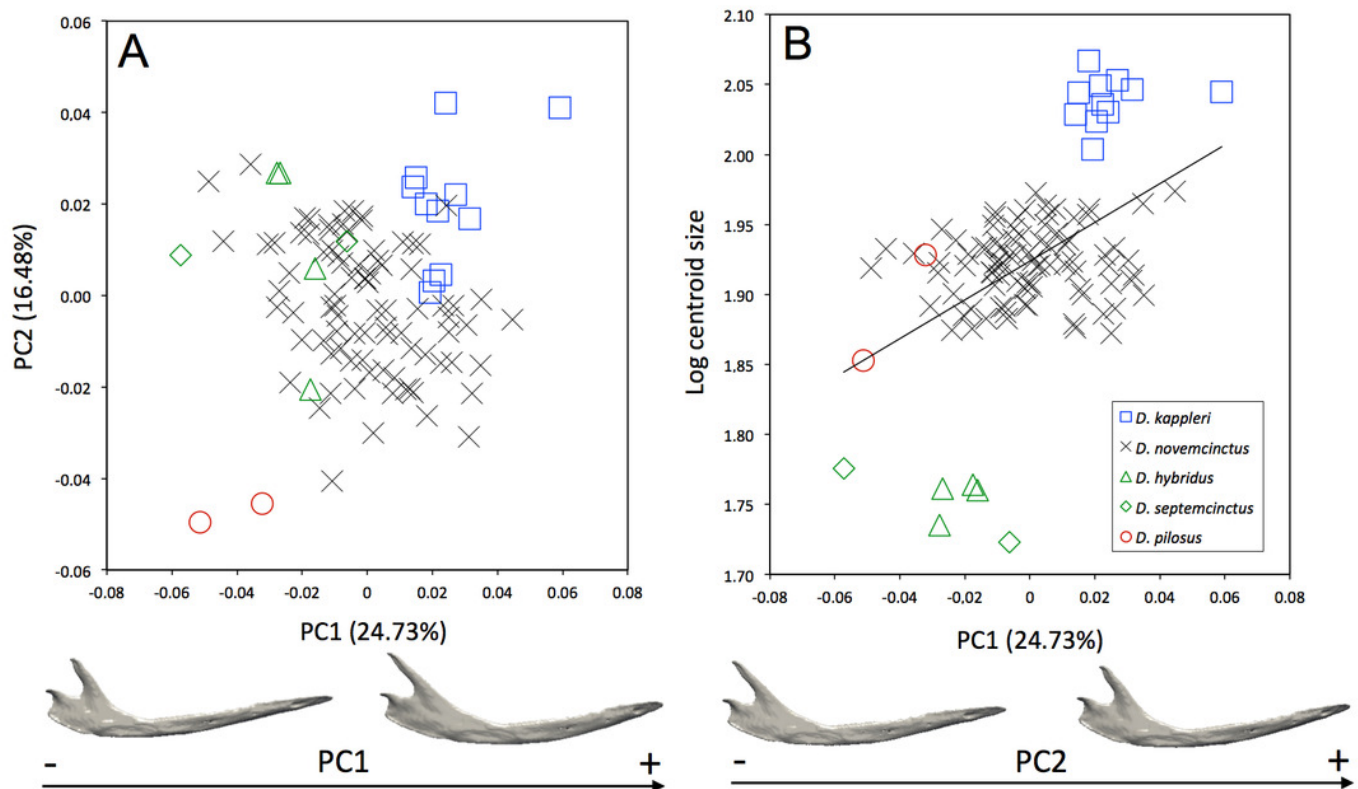


# Figure 4

Figure 4

(A) Principal component analysis (PC1 vs PC2) and associate patterns of morphological transformation for crania of five *Dasypus* species. (B) Regression of the first principal component on the logarithm of the centroid size ( $R^2=0.55$ ;  $p<0.001$ ). Symbols: blue squares, *D. kappleri*; black crosses, *D. novemcinctus*; green triangles, *D. hybridus*; green diamonds, *D. septemcinctus*; red circles, *D. pilosus*.

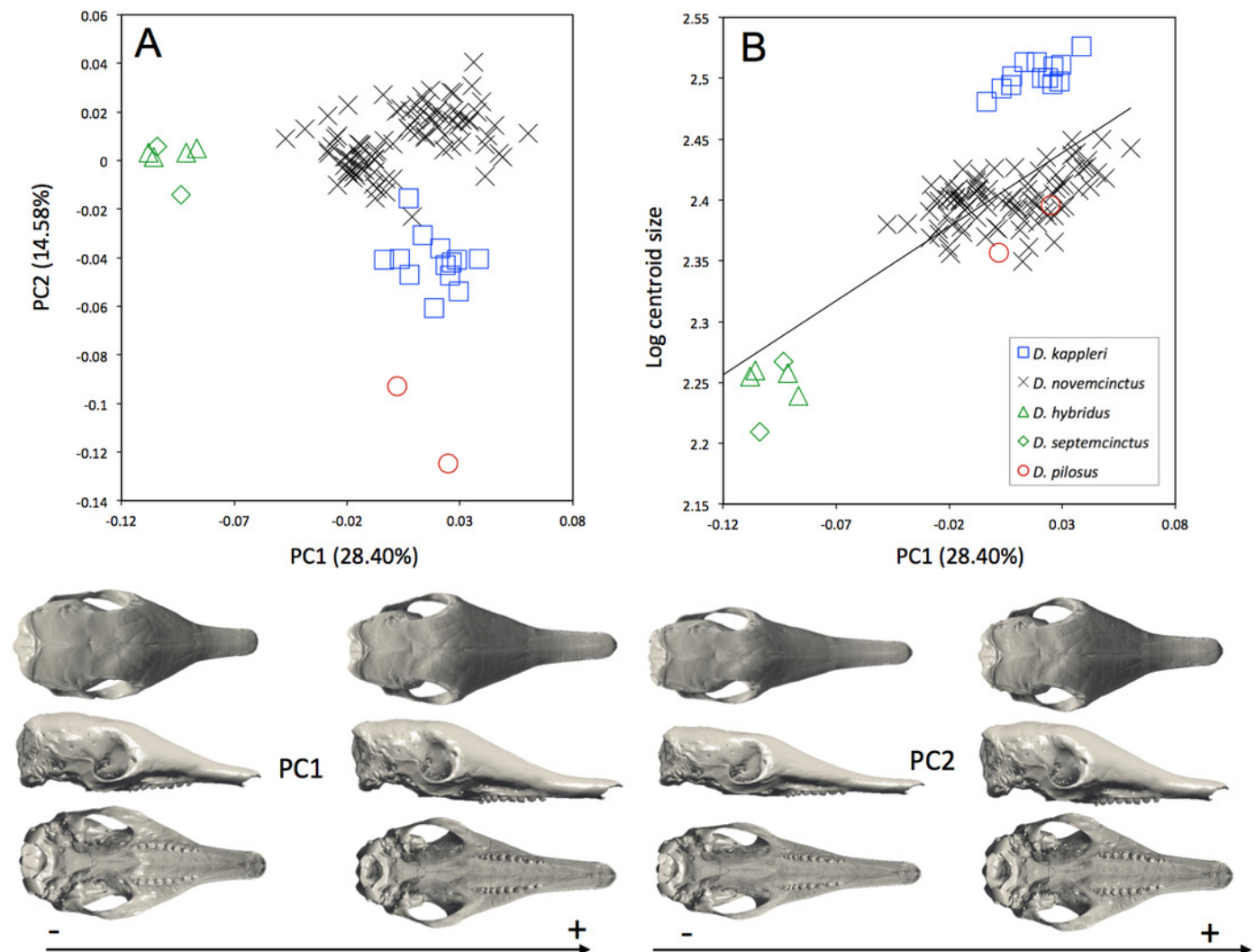


# Figure 5

Figure 5

**(A)** Principal component analysis (PC1 vs PC2) and associate patterns of morphological transformation for mandibles of *Dasypus novemcinctus*. **(B)** Regression of the first principal component on the logarithm of the centroid size ( $R^2=0,035$ ;  $p=0.03$ ). *Symbols:* green diamonds, Bolivia; green triangle, Brazil (solid green triangles are for specimens from Amapa); green circles, Paraguay; green crosses, Peru; green squares, Uruguay; green bars, Venezuela; blue diamonds, Belize; blue “plus”, Guatemala; blue bars, Honduras; Blue squares, Mexico; blue crosses, Nicaragua; blue triangles, USA; blue circles, Costa Rica; black triangles, Colombia; black crosses, Ecuador; black stars, Panama; orange squares, French Guiana; orange crosses, Guyana; orange circles, Suriname.

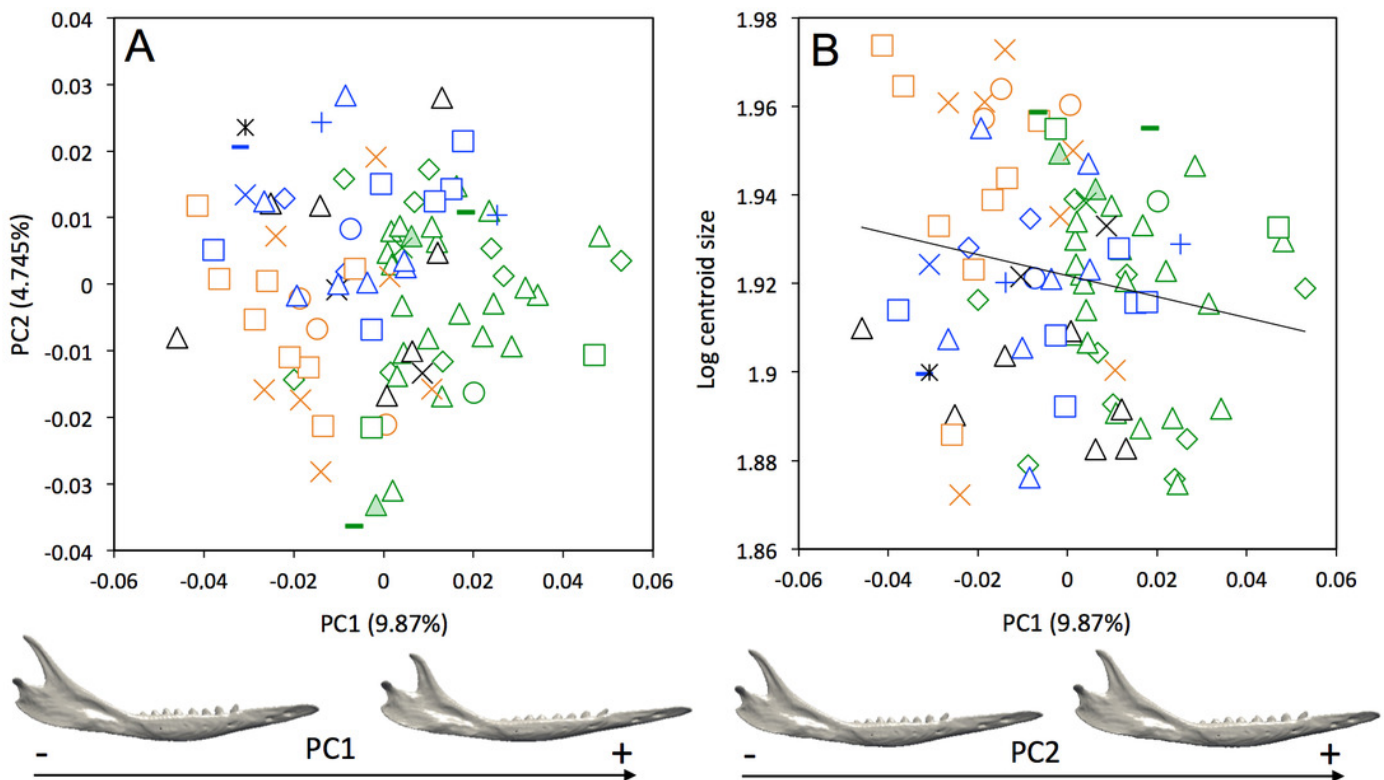


## Figure 6

### Figure 6

Principal component analysis (**A**, PC1 vs PC2; **B**, PC3 vs PC4) and associate patterns of morphological transformation for crania of *Dasypus novemcinctus*. *Symbols*: green diamonds, Bolivia; green triangle, Brazil (solid green triangles are for specimens from Amapa); green circles, Paraguay; green crosses, Peru; green squares, Uruguay; green bars, Venezuela; blue diamonds, Belize; blue “plus”, Guatemala; blue bars, Honduras; Blue squares, Mexico; blue crosses, Nicaragua; blue triangles, USA; blue circles, Costa Rica; black triangles, Colombia; black crosses, Ecuador; orange squares, French Guiana; orange crosses, Guyana; orange circles, Suriname.

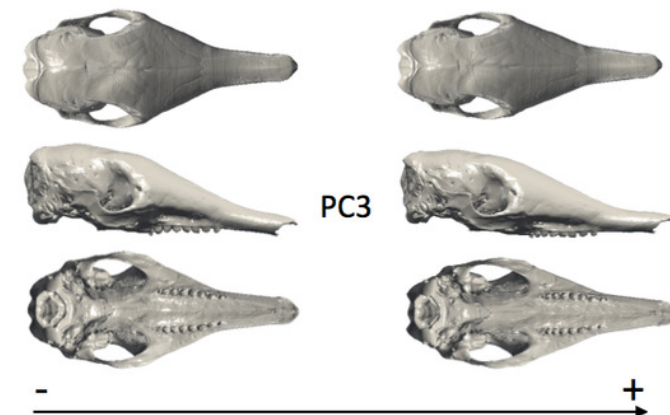
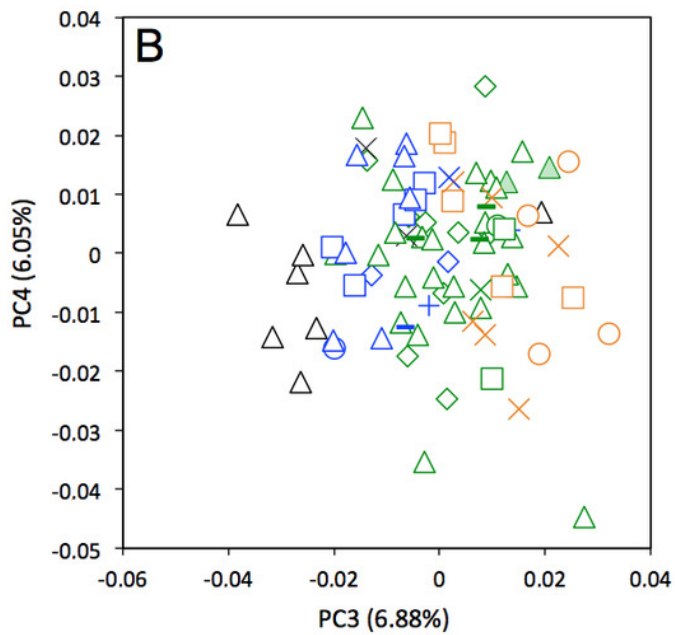
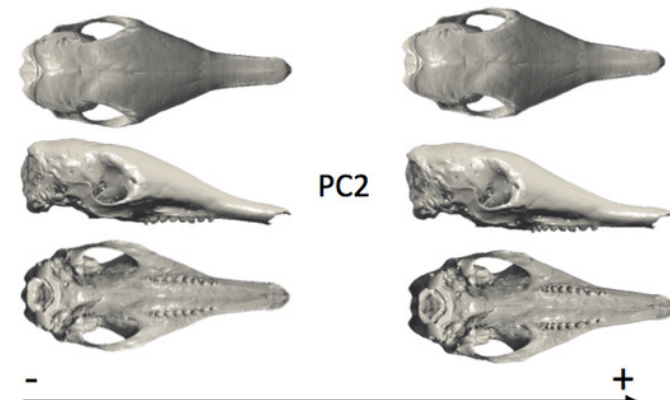
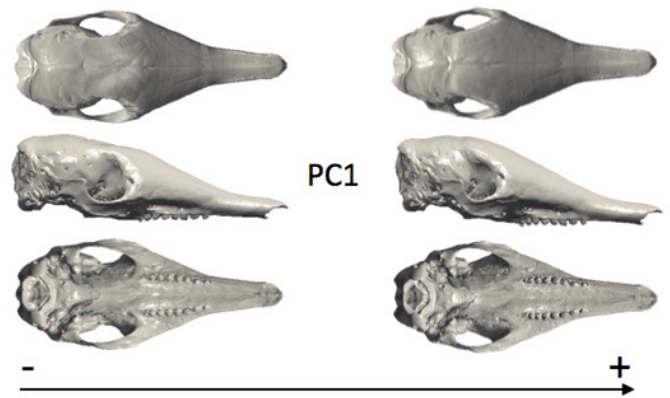
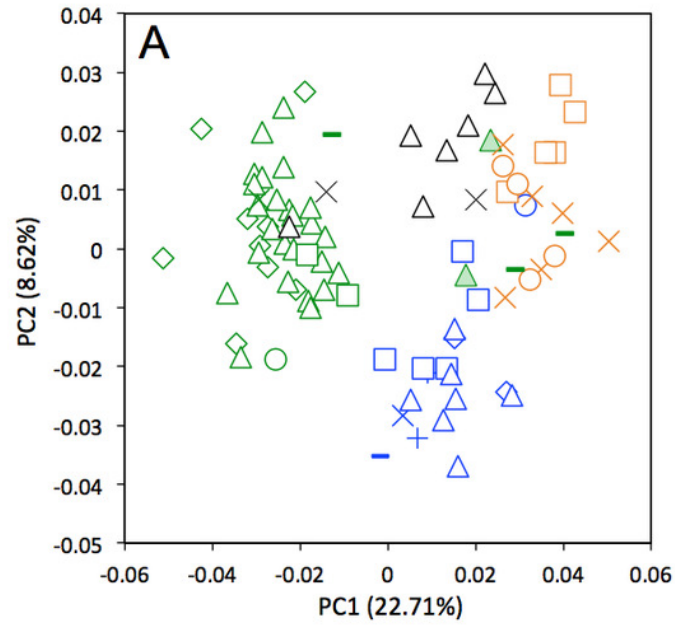


## Figure 7

### Figure 7

Regression of the first cranial principal component (*Dasypus novemcinctus*) on the logarithm of the centroid size ( $R^2=0.15$ ;  $p<0.001$ ). *Symbols*: green diamonds, Bolivia; green triangle, Brazil (solid green triangles are for specimens from Amapa); green circles, Paraguay; green crosses, Peru; green squares, Uruguay; green bars, Venezuela; blue diamonds, Belize; blue “plus”, Guatemala; blue bars, Honduras; Blue squares, Mexico; blue crosses, Nicaragua; blue triangles, USA; blue circles, Costa Rica; black triangles, Colombia; black crosses, Ecuador; orange squares, French Guiana; orange crosses, Guyana; orange circles, Suriname.



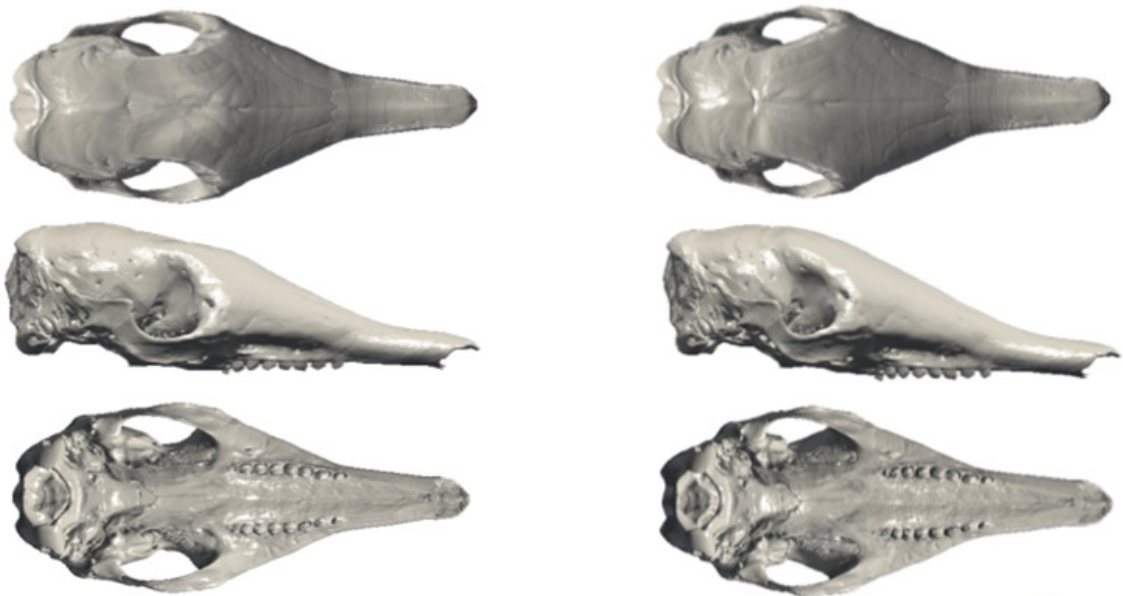
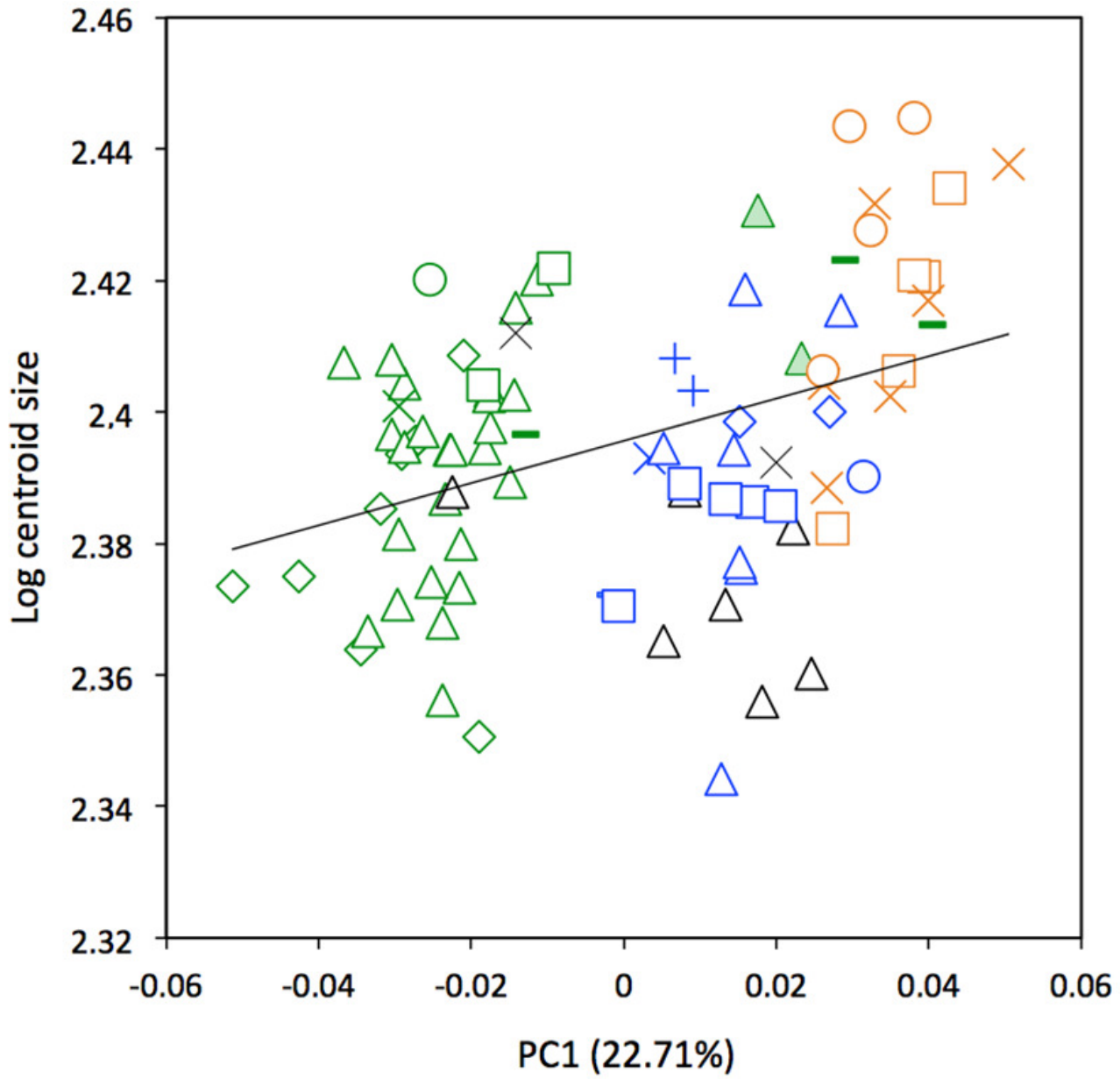


# Figure 8

Figure 8

Linear Discriminant Analysis (LDA) performed on cranial shape coordinates of *Dasyops novemcinctus*. Symbols: green diamonds, Bolivia; green triangle, Brazil (solid green triangles are for specimens from Amapa); green circles, Paraguay; green crosses, Peru; green squares, Uruguay; green bars, Venezuela; blue diamonds, Belize; blue “plus”, Guatemala; blue bars, Honduras; Blue squares, Mexico; blue crosses, Nicaragua; blue triangles, USA; black triangles, Colombia; black circles, Costa Rica; black crosses, Ecuador; orange squares, French Guiana; orange crosses, Guyana; orange circles, Suriname.

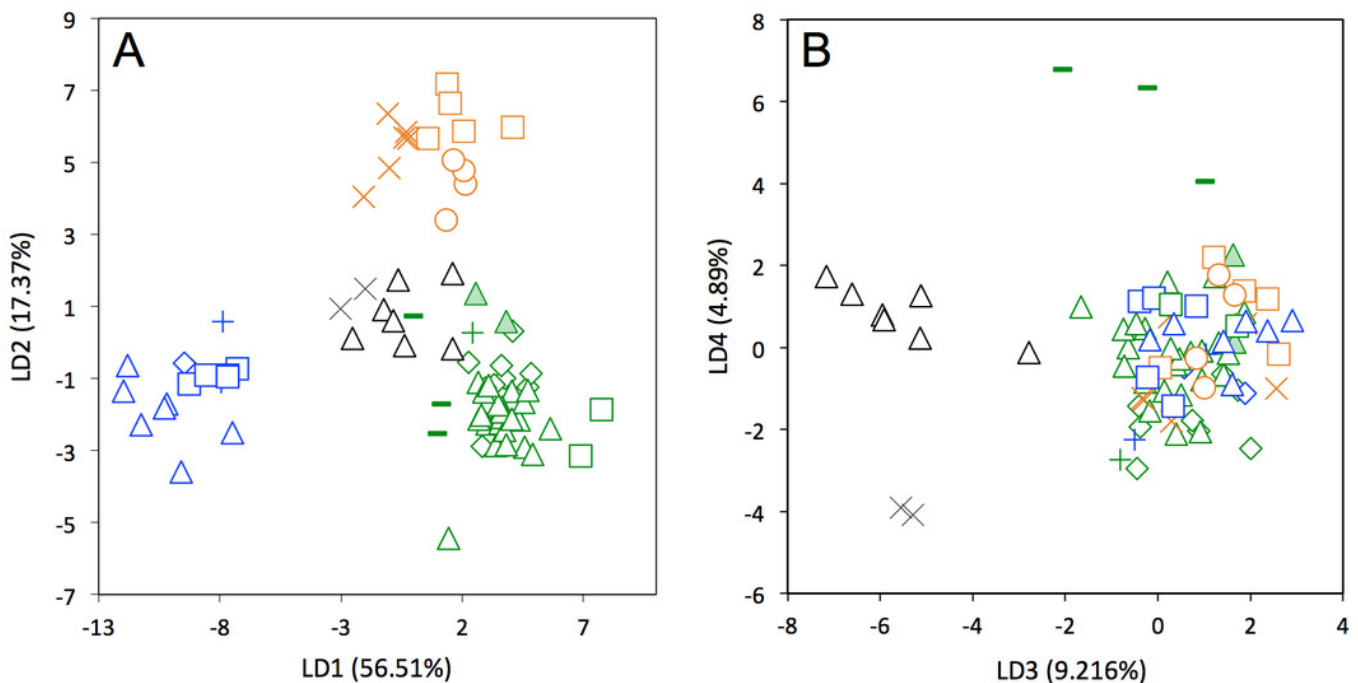




# Figure 9

Figure 9

Summary map showing the geographical distribution of nine-banded armadillo specimens investigated in this study and their attribution to one of the four main morphotypes defined in this study: black, Central group; blue, Northern group; green, Southern group; orange, Guianan group. Specimens lacking precise geographical information (other than country of origin) are indicated with a square.

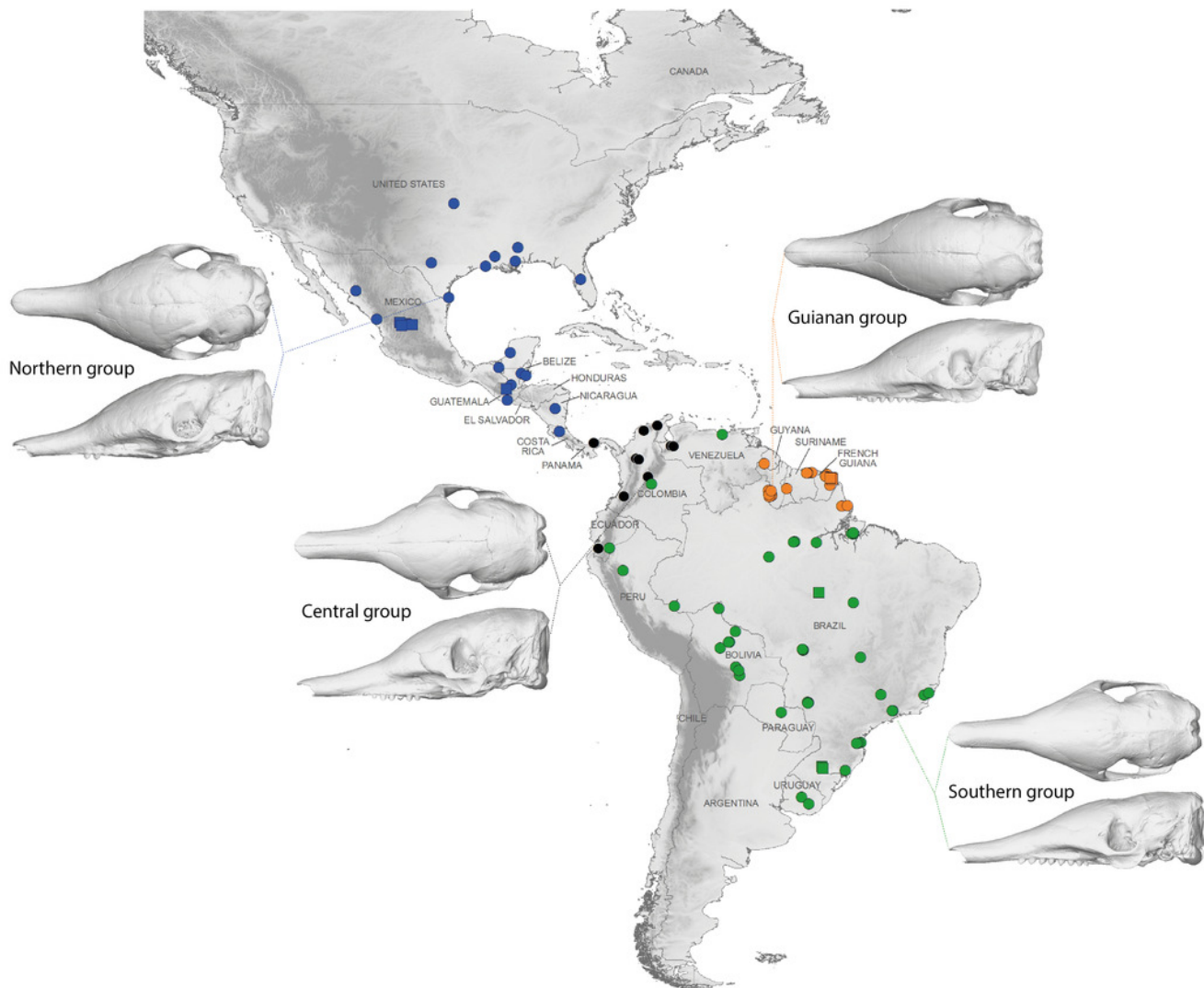


**Table 1** (on next page)

Table 1

Definitions of the landmarks used on the mandible

---

<b>Numbers</b>	<b>Definition</b>
1	Most anterior point of the mandible
2	Most anterior point of the alveolar margin of the tooth row
3	Most posterior point of the seventh tooth
4	Tip of the coronoid process
5	Point at the maximum of concavity between the coronoid and the condyloid processes
6	Most lateral point of the articular surface of the condyle
7	Most medial point of the articular surface of the condyle
8	Point at the maximum of concavity between the condyloid and the angular
9	Tip of the angular process
10	Mandibular foramen

---

1

**Table 2** (on next page)

## Table 2

Definitions of the landmarks used on the cranium. Landmarks indicated with a star were not used in the intraspecific comparisons.

Numbers	Definition
1	Most anterodorsal point of the nasal suture
2	Intersection between inter-nasal and inter-frontal sutures
3	Intersection between inter-parietal and inter-frontal sutures
4	Intersection between inter-parietal and supra-occipital
5	Most distal point of the supra-occipital
6 and 7	Intersection between frontal, maxillar, and nasal sutures
8 and 9	Most dorsomedial point of the orbit (i.e. minimal interorbital length)
10 and 11	Most posterolateral point of the supra-occipital
12 and 28	Most anterolateral point of the premaxillar/nasal suture
13 and 29	Intersection between premaxillar, maxillar, and nasal sutures
14 and 30	Intersection between the lacrimal, maxillar, and frontal sutures
15 and 31	Anteroventral margin of the lacrimal foramen
16 and 32	Anteroventral margin of the upper ethmoid foramen
17 and 33	Most anterior point of the squamosal, frontal, and alisphenoid sutures
18 and 34	Most dorsal point of the maxillary foramen
19 and 35	Most dorsal point of the infraorbital foramen
20 and 36	Most anteroventral point of the sphenopalatine fissure
21 and 37	Most dorsal point of the jugal/maxillar suture
22 and 38	Most dorsal point of the jugal/squamosal suture
23 and 39	Most posterior point of the postglenoid process
24 and 40	Most posterodorsal point of the zygomatic part of the squamosal
25 and 41	Intersection between the frontal, squamosal, and parietal sutures
26 and 42	Most dorsal point of sulcus for external acoustic meatus on squamosal
27 and 43	Intersection between the parietal, squamosal, and supraoccipital sutures
44 and 60	Most posterior point of the premaxillar/maxillar suture in ventral view
45 and 61	Most anterior point of the alveolar margin of the tooth row
46 and 62	Most posterior point of the alveolus of the seventh dental locus
47 and 63	Intersection between the lacrimal/maxillar suture and the zygomaseteric crest in ventral view
48	Intersection between maxillar and palatine sutures
49 and 64	Most posterolateral point of the pterygoid wings
50 and 65	Transverse canal foramen
51 and 66	Most anterodorsal point of the <i>foramen ovale</i>
52 and 67	Most ventral of the alisphenoid/squamosal suture
53 and 68	Most lateral point between the basioccipital/basisphenoid sutures
54 and 69	Most posterolateral point of the jugular foramen
55 and 70	Most posterolateral point of the hypoglossal foramen
56 and 71	Most anterolateral point of the occipital condyle
57 and 72	Intersection between the basioccipital, the occipital condyle, and the <i>foramen magnum</i>
58	Most antero-ventral point of the <i>foramen magnum</i>
59	Most postero-dorsal point of the <i>foramen magnum</i>
73 and 74	Intersection between the supraoccipital, exoccipital, and petrosal sutures
75 and 76	Most posterior point of the postglenoid foramen
77 and 78	Caudal palatine foramen
79* and 80*	Point of maximum concavity on the maxillar/frontal suture in dorsal view
81 and 82	Intersection between the lacrimal/frontal suture and the orbit
83	Most posterior point of the frontal sinuses in the midline
84	Ventral tip of the tentorial process